Northern Illinois University

Signal-background interference for digluon resonances at the Large Hadron Collider

Prudhvi Bhattiprolu[†]

(pbhattiprolu@niu.edu)

[†] Northern Illinois University

Phenomenology Symposium
May 4th, 2020

Based on work with Steve Martin, arXiv:hep-ph/2004.06181

Dijet resonances

New physics $\xrightarrow{?}$ gg, $q\bar{q}$, qq, or qg

Some models[†] of interest that yield dijet signals:

- Chiral color
- Flavor-universal coloron
- certain SUSY models

} predict massive color-octet gauge bosons[‡]

- Some E_6 GUTs predict diquarks
- Models with new electroweak gauge bosons W' and Z'
- Excited or composite quark models
- String Regge resonances of the quark and the gluon
- Randall-Sundrum (RS) model
- Kaluza-Klein (KK) models

} predict massive gravitons

- Models with dark matter mediators which also couple to quarks

[†] See e.g. T. Han, I. Lewis, Z. Liu 1010.4309, and references therein.

[‡] These are known as **axigluons** (axial-vectors) or **colorons** (vectors) or **topgluons**. In these models, QCD is embedded within a broken symmetry of $SU(3) \times SU(3)$ gauge group beyond the TeV scale.

"Anti"-Motivation for bump hunting

In the searches for dijet resonances,

$$\text{Full signal} \begin{cases} = \text{(Resonant) Signal} + \text{QCD Interference} \\ \neq \text{(Resonant) Signal} \end{cases}$$

The dijet resonances need not necessarily produce a peak in the dijet mass distributions in the vicinity of their mass, which implies that

> Resonance hunting is not the same as bump hunting.

The interference between the resonant amplitude and the QCD background was not considered while setting limits on dijet resonances in the LHC searches.[†]

[†] The most recent ones can be found in 1806.00843, 1911.03947 (CMS) and 1703.09127, 1910.08447 (ATLAS).

Digluon resonances

Here and from now on, X refers to any digluon resonance.

We studied the importance of the interference[†] between the digluon resonant signal $gg \to X \to gg$ and the QCD background $gg \to gg$ for:

- Spin 0, color singlet[‡]
- Spin 0, color octet
- Spin 1, color octet
- Spin 2, color singlet

where X couples to gluon pairs by non-renormalizable operators invariant under QCD gauge transformations.

[†] The interference effects are likely to be most pronounced in the digluon channel, where the QCD background amplitudes are large compared to the new-physics amplitudes.

[‡] A preliminary study of this kind, for spin-0 color-singlets, done only at parton level with smearing, was performed in S. P. Martin 1606.03026.

Feynman rules

Feynman rules, for X-g-g coupling, for a spin-0 color-singlet:

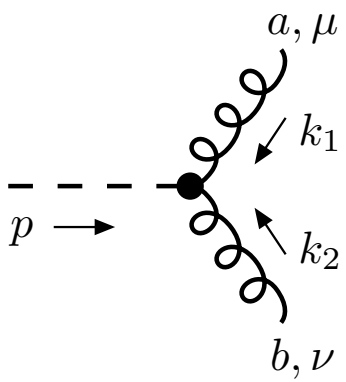

$$-i\frac{2c_1}{\Lambda}\delta^{ab}(k_1\cdot k_2\,\eta^{\mu\nu} - k_2^{\mu}k_1^{\nu}) \qquad \text{(scalar)}$$

$$-i\frac{2c_2}{\Lambda}\delta^{ab}\epsilon^{\mu\nu\rho\sigma}k_{1\rho}k_{2\sigma} \qquad \text{(pseudo-scalar)}$$

Here, c_i are dimensionless form factors[†], and Λ is the mass scale associated with the new physics.

The other spin and color choices for X have very different Lorentz and QCD index structures, which as we will see will be important later.

[†] The effective form-factor couplings will be suppressed by masses of heavier particles, if the interaction is loop-induced.

Benchmark models

Resonance Mass M_X (GeV)	$\Gamma^2_{gg}/\Gamma M_X$			
	$J = 0$, singlet	$J = 0$, octet	$J = 1$, octet	$J = 2$, singlet
750	0.0015	0.00016	0.00005	0.0003
1000	0.002	0.0002	0.000065	0.00041
1500	0.005	0.0005	0.00015	0.001
2000	0.019	0.0018	0.00054	0.00375
2500	0.0108	0.001	0.0003	0.0022
3000	0.07	0.006	0.00183	0.014

Here M_X, Γ, and Γ_{gg} are the mass, total width, and digluon partial width of X, respectively.

We chose benchmark models in the above table such that the s-channel resonant-only cross sections are close to the claimed exclusions by CMS in 1806.00843, 1911.03947.

LO partonic differential cross-sections

LO partonic differential cross-section:[†‡§]

$$\frac{d\hat{\sigma}}{dz} = \frac{d\hat{\sigma}_s}{dz} + \frac{d\hat{\sigma}_t}{dz} + \frac{d\hat{\sigma}_u}{dz} + \frac{d\hat{\sigma}_{s,t}}{dz} + \frac{d\hat{\sigma}_{t,u}}{dz} + \frac{d\hat{\sigma}_{s,u}}{dz} + \frac{d\hat{\sigma}_{s,QCD}}{dz} + \frac{d\hat{\sigma}_{t,QCD}}{dz} + \frac{d\hat{\sigma}_{u,QCD}}{dz}.$$

z: cosine of the gluon scattering angle in the partonic COM frame.

LO digluon production cross section at the LHC ($\sqrt{s} = 13$ TeV):

$$\frac{d\sigma_{pp\to gg}}{d(\sqrt{\hat{s}})} = \sqrt{\hat{s}} \int_{x_-}^{x_+} \frac{dx}{xs} g(x) g\left(\frac{\hat{s}}{xs}\right) \int_{-z_{\rm cut}}^{z_{\rm cut}} dz \frac{d\hat{\sigma}}{dz}.$$

x: longitudinal momentum fraction for the parton

$g(x)$: gluon PDFs

$\sqrt{\hat{s}} = m_{gg}$: digluon invariant mass in both initial and final states

---

[†] Excluding the pure QCD contribution.

[‡] $d\hat{\sigma}_{s,QCD}/dz$, for example, stands for the interference of the s-channel X exchange diagram with the pure QCD amplitude

[§] For more details, see slides 36-38. $d\hat{\sigma}/dz$ for all the digluon resonances considered are shown in slides 39-42

The wide jet algorithm[†]

- All jets should satisfy an object cut $|\eta_j| < 2.5$.
- Start with the two leading p_T jets.
- All p^{μ}_{jet} within $\Delta R = \sqrt{(\Delta\eta)^2 + (\Delta\phi)^2} < 1.2$ of two leading p_T jets are added to the nearest leading jet to obtain two wide jets.
- These wide jets should satisfy $p_{T_j} > p_{T_j}^{\text{wide-jets}} = 100$ GeV.
- Additionally,

$$|\Delta\eta_{jj}| \quad < \quad \begin{cases} 1.3 \text{ (for } M_X < 1800 \text{ GeV, CMS 1806.00843)} \\ 1.1 \text{ (for } M_X > 1800 \text{ GeV, CMS 1911.03947)} \end{cases}$$

  tends to improve the efficiency for pure resonance events compared to interference.[‡]

[†] We follow the procedure used by CMS (1806.00843, 1911.03947) to reduce the sensitivity to radiation of additional gluons from the final state gluons.

[‡] However, this certainly does not reduce the effects of interference to a negligible level.

Showering, hadronization, and detector-level simulation

Events for resonant signal and interference were generated (at LO) by:
FeynRules v2.3 → MadGraph v2.6.6 → Pythia 8.2 → Delphes 3.4.

For dijet mass distributions, we obtain the dijet mass (m_{jj}) of two "wide jets", obtained using the wide jet algorithm.[†]

Challenges to generate dijet mass distributions for the interference terms:

- Negative cross-sections (event weights in *.lhe* file)
- The color flow problem (only for **color-singlets**)

[†] See Slide 8

Challenges: Negative cross-sections

Simply generating a full QCD+X sample and then subtracting the pure QCD part is not practical, because of the very poor statistics.[†]

Instead, the following works:

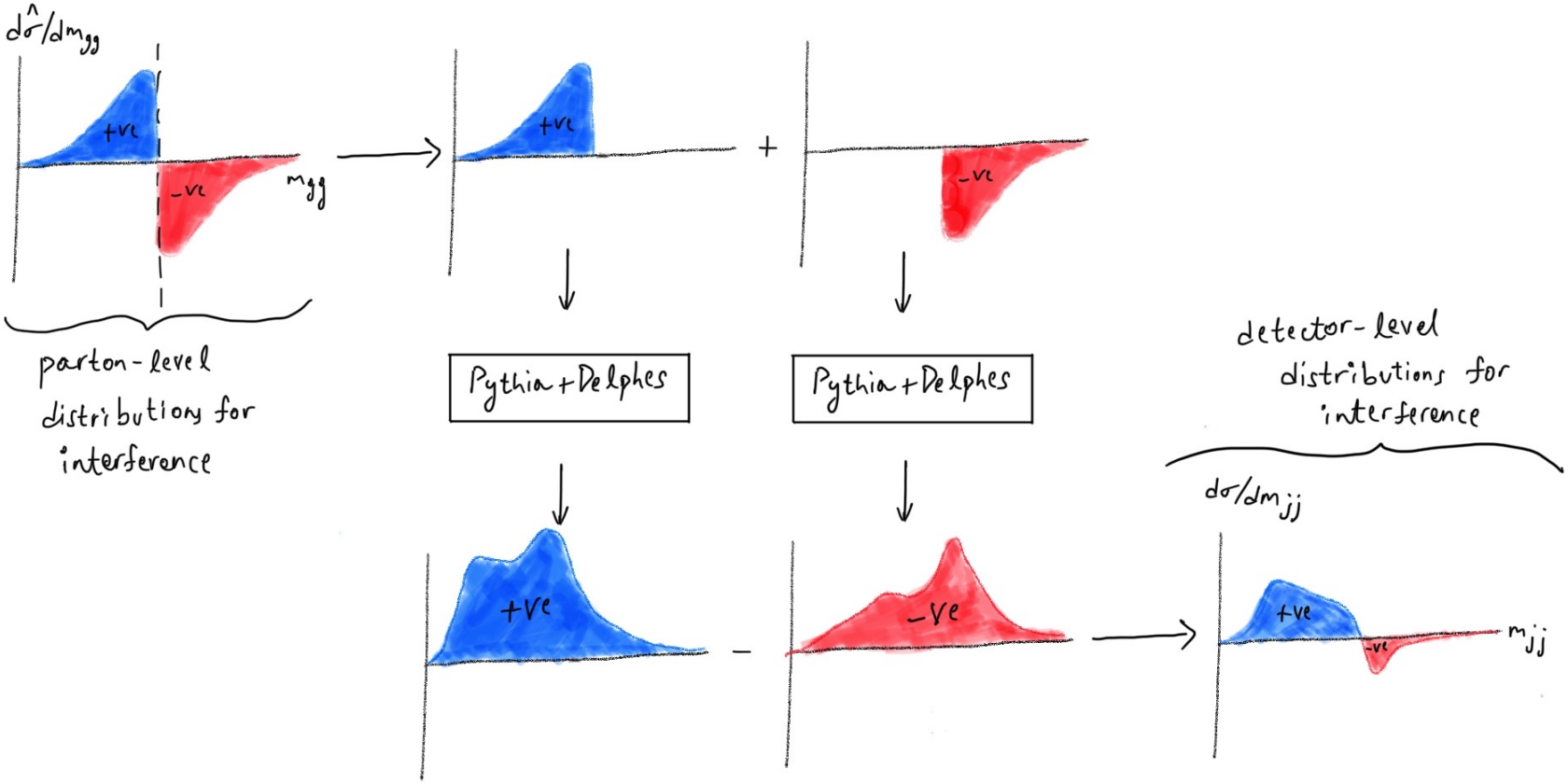

[†] The actual LHC experiment has much better statistics than our simulations can provide.

Interlude: Color flow

For event simulations, color is treated by "color flow" which is given by integer tag entries for "color flow" lines, for each parton-level event.[†]

The integer tags (e.g. 1-4) for the color flow lines are required by the showering and hadronization event generators (e.g. PYTHIA[‡]) to begin the parton shower.

Example:

Color flow for $gg \to gg$ (t/u-channel, QCD)

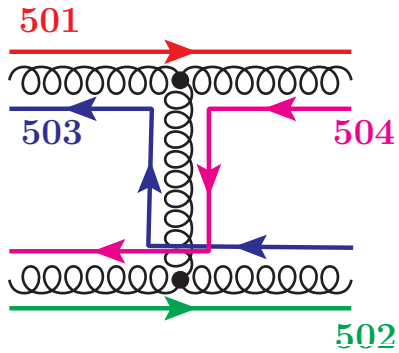

I	ISTUP(I)	IDUP(I)	MOTHUP(1,I)	MOTHUP(2,I)	ICOLUP(1,I)	ICOLUP(2,I)
1	−1	21 (g)	0	0	501	503
2	−1	21 (g)	0	0	502	504
3	+1	21 (g)	1	2	501	504
4	+1	21 (g)	1	2	502	503

[†] See e.g. E. Boos *et al.* hep-ph/0109068; F. Maltoni, K. Paul, T. Stelzer, S. Willenbrock hep-ph/0209271; M. E. Peskin `http://hep.ps.uci.edu/~wclhc07/PeskinIrvine.pdf`

[‡] The integer tags are typically assigned as 501-504 in PYTHIA

Challenges: The color flow problem

MADGRAPH cannot assign a color flow for each parton-level event for the interference between the QCD background and color-singlet digluon resonant signal. Without a color flow choice, PYTHIA cannot run.

To get around this:

We generated detector-level events for the color-singlet interferences by simply assigning a color flow "by hand" to each parton-level event.

4 physically distinct color flow possibilities[†] $\rightarrow$ 4 results $\rightarrow$ spread of possible differential cross-sections.

On the other hand, this problem does not occur for color-octets.

[†] See Slide 13

Color flows for color-singlet interferences (with QCD)

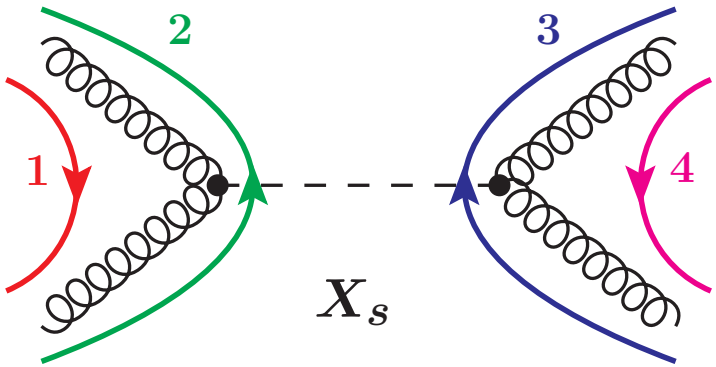

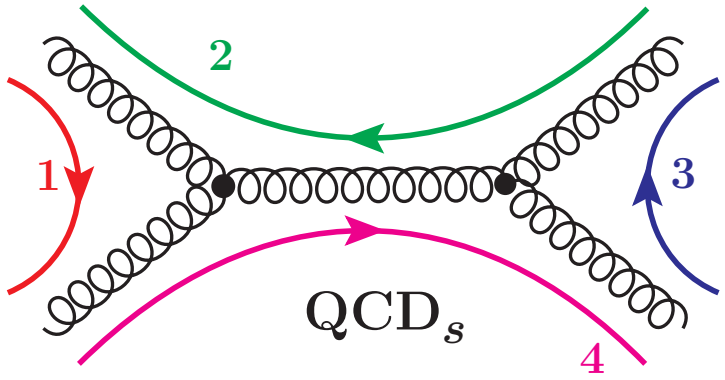

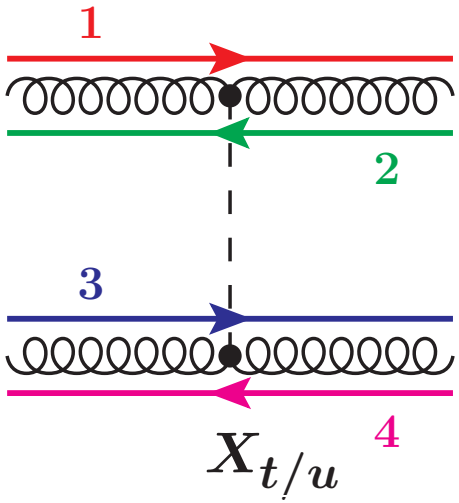

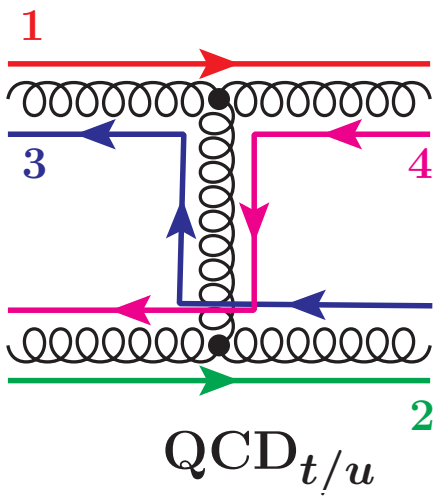

Results for $\Gamma = \Gamma_{gg}$: Spin 0, color singlet (Monte Carlo simulations)

Since there are four physically distinct color flow possibilities, we obtain four distributions for the full results (with interference).

$M_X = 1000$ GeV

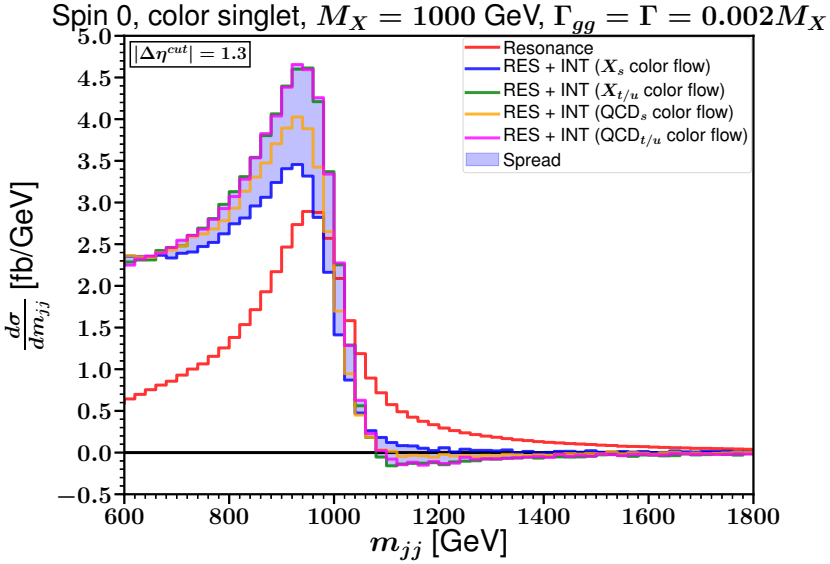

$M_X = 3000$ GeV

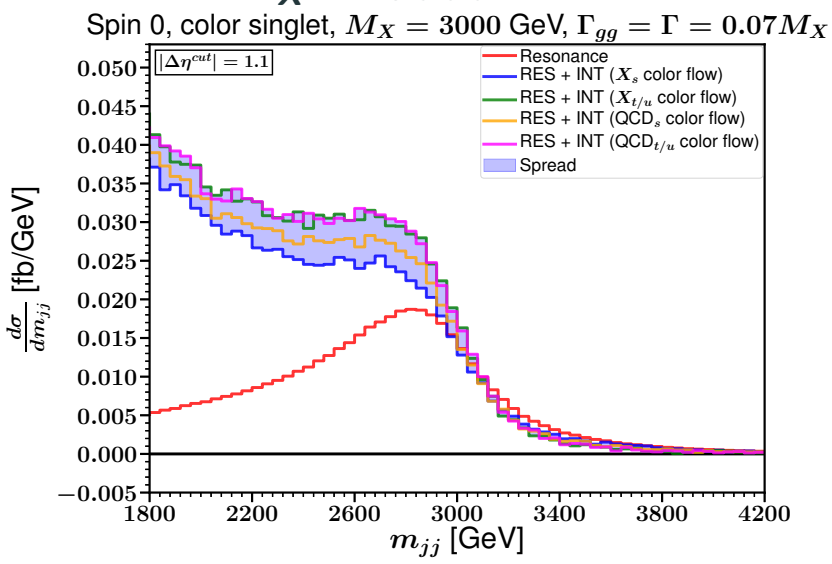

- Large low-mass tail below M_X, and deficit of events above M_X compared to resonance-only results.
- Relative importance of interference seems to increase with resonance mass.
- After QCD background fit, might see an effective dip or peak/dip.

A quick cross-check: Spin 0, color singlet†

$M_X = 1000$ GeV:

Smeared partonic

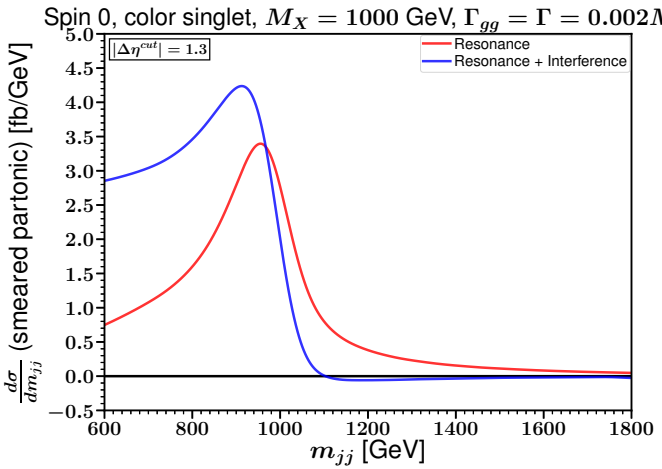

Simulated

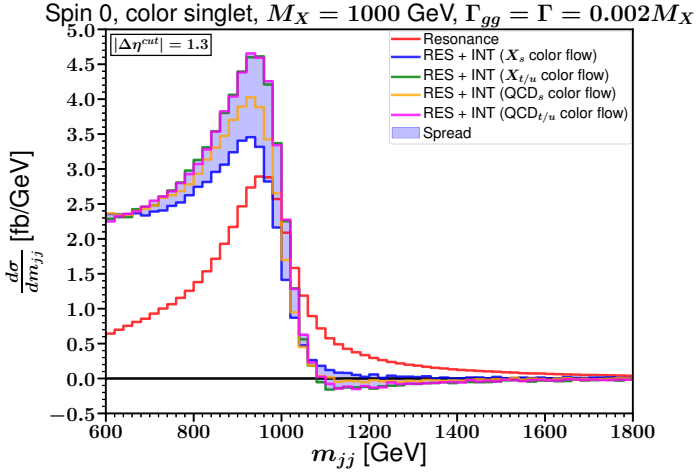

$M_X = 3000$ GeV:

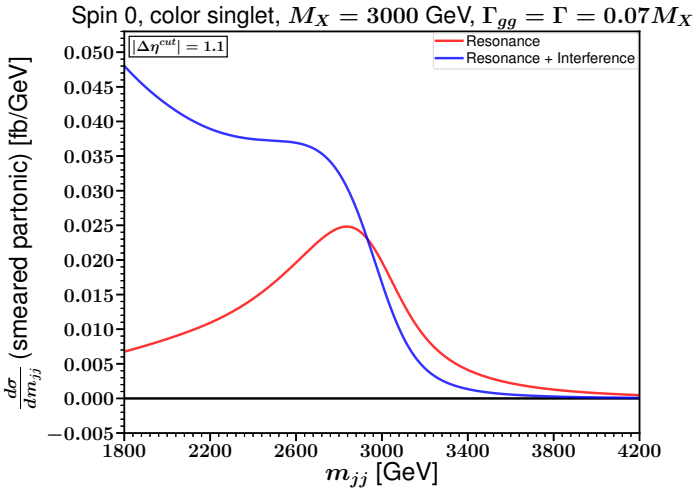

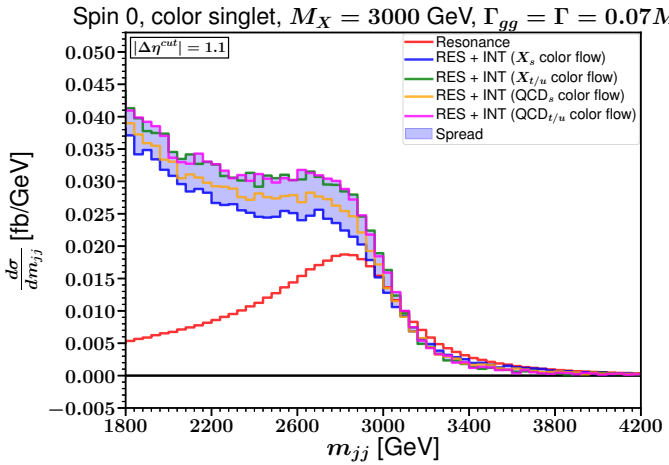

† Plots in the left-column are obtained by parton-level analysis with smearing [see slide 44].

Results for $\Gamma = \Gamma_{gg}$: Spin 0, color octet (Monte Carlo simulations)

Unlike the case of a color-singlet scalar, here we have exactly one result for the QCD interferences because the color flow is uniquely determined.

$M_X = 1000$ GeV

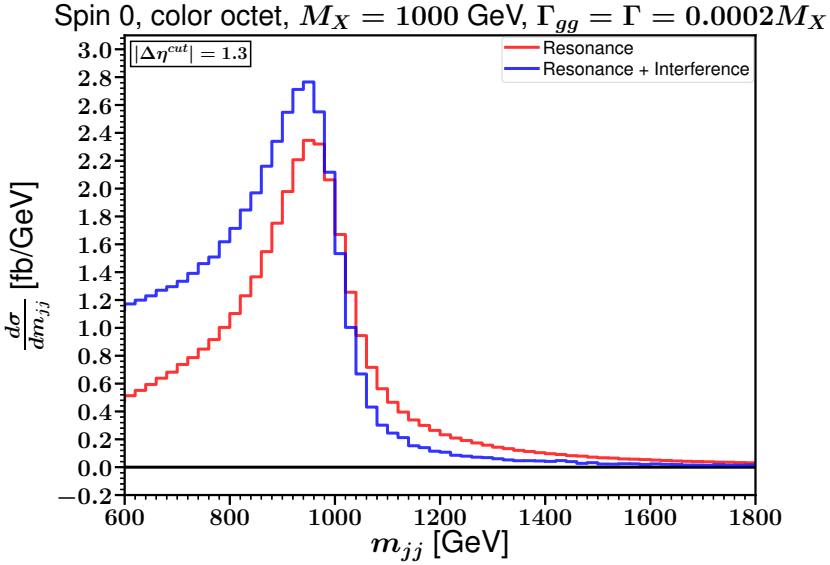

$M_X = 3000$ GeV

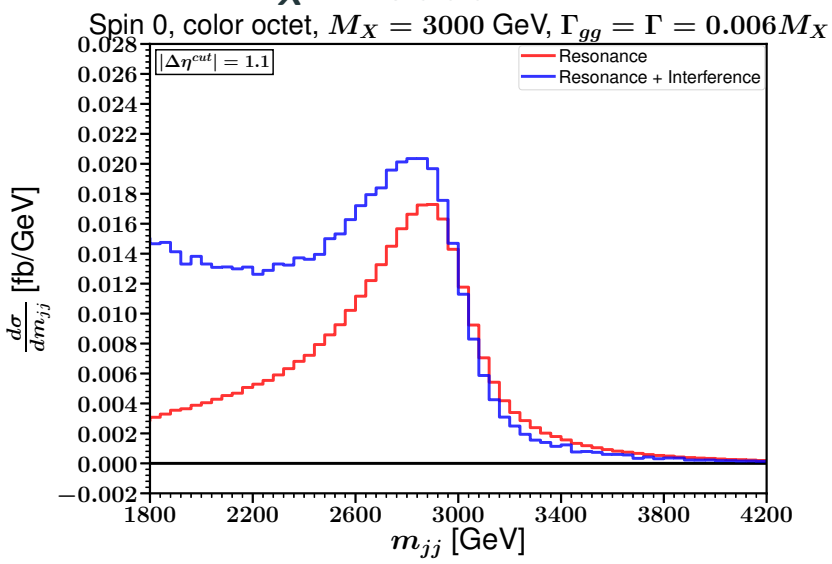

- Main feature is again large low-mass tail.
- Interference effects not as big as for color-singlet scalars.
- QCD background fitting might lead to peak/dip or pure dip.

Results for $\Gamma = \Gamma_{gg}$: Spin 1, color octet (Monte Carlo simulations)

Again, we have exactly one result for the QCD interferences because the color flow is uniquely determined.

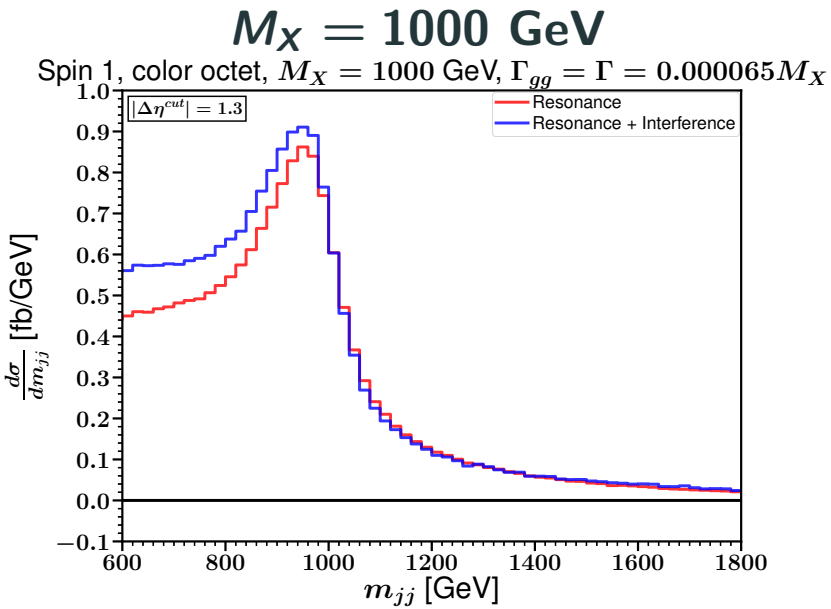

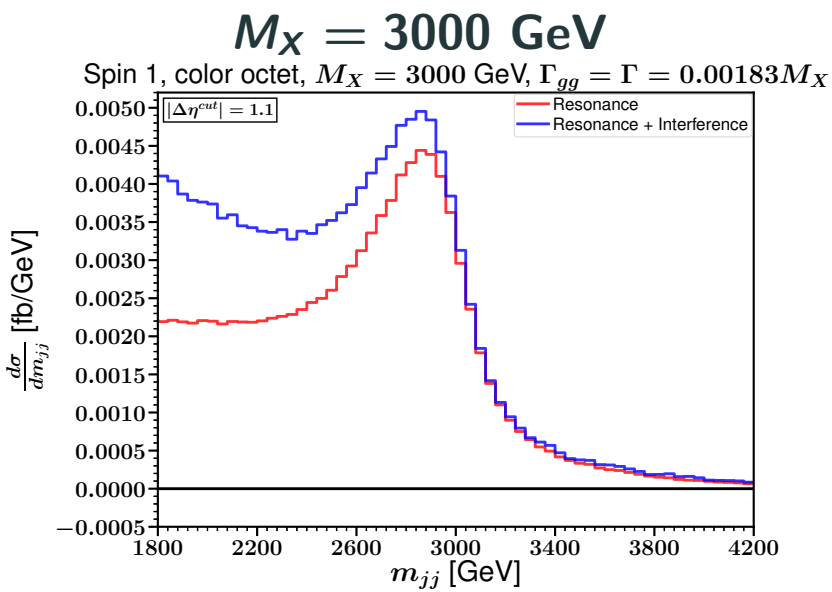

- Results for $m_{jj} > M_X$ almost unaffected by including the interference.
- Large low-mass tail, getting larger with M_X.
- After QCD background fit, might see an apparent dip.

Results for $\Gamma = \Gamma_{gg}$: Spin 2, color singlet (Monte Carlo simulations)

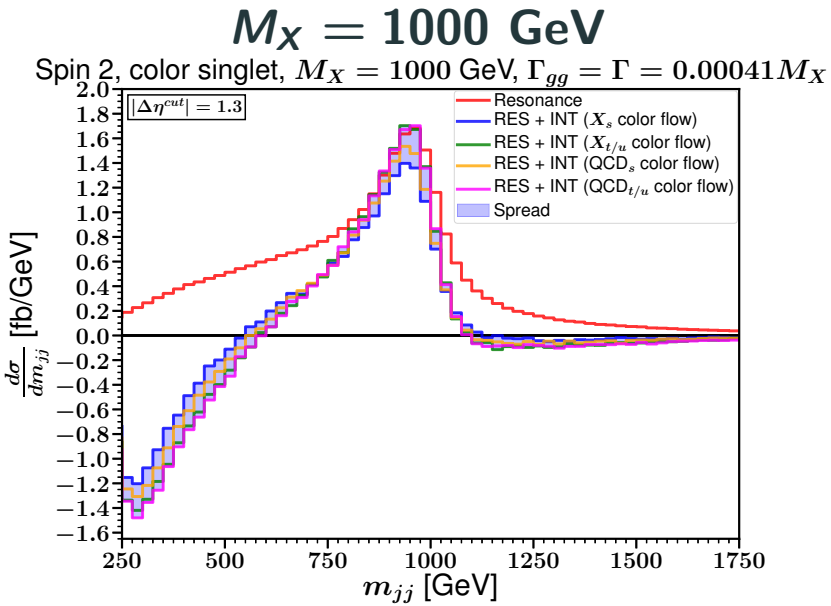

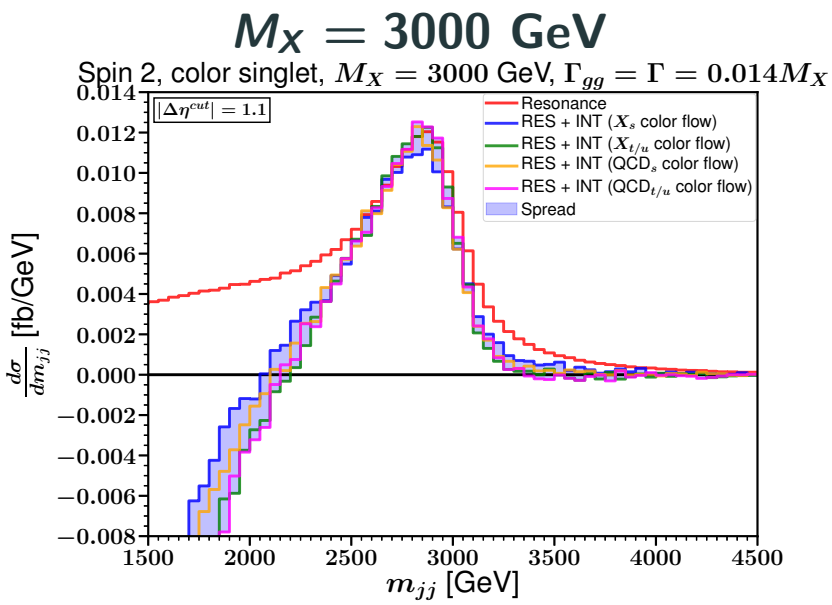

- Large negative low-mass tail, and it comes from the interference between t- and u-channel X exchange diagrams and QCD.
- QCD background fitting might lead to an enhancement of the peak compared to naive resonance-only distribution.

Additional checks

We checked the following:

- The interference effect would have been larger without the $\Delta\eta$ cut.
- Parton-level distributions obtained using MADGRAPH (not shown here) closely match the parton-level distributions obtained by our calculations.
- The relative impact of the interference stays nearly constant for a fixed M_X as the resonant cross-section decreases.
- The interference effects are relatively enhanced[‡] for the general case with $\Gamma_{gg} < \Gamma$, compared to the case with $\Gamma = \Gamma_{gg}$.

[†] The reason for this is that to reach the same cross-section, both Γ_{gg} and Γ must be larger than if they were equal [see eq. on Slide 28], leading to much larger Breit-Wigner tails away from the resonance region, which then produce larger interference with the QCD amplitude [see slides 55-59 for the results for $\Gamma = 5\Gamma_{gg}$].

Results for $\Gamma = 5\Gamma_{gg}$: Spin 0, color singlet (Monte Carlo simulations)

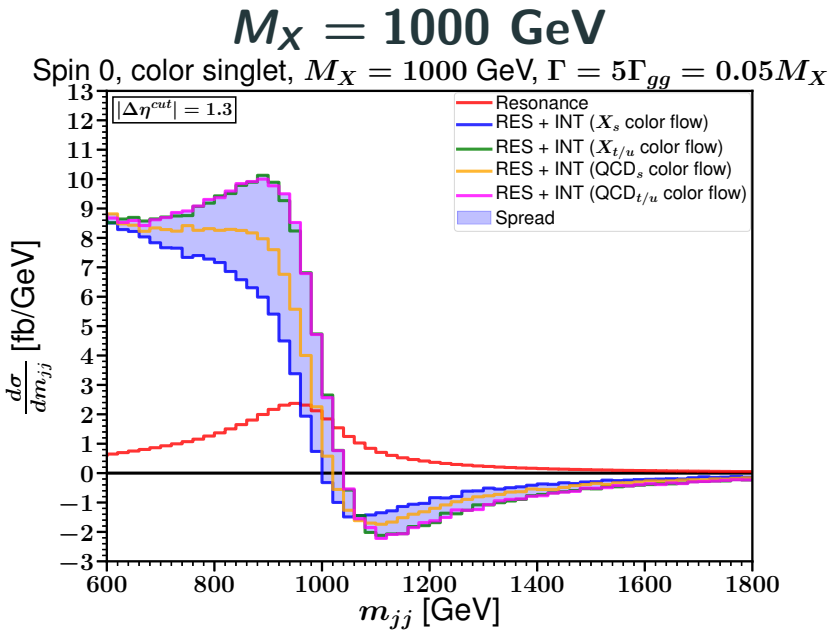

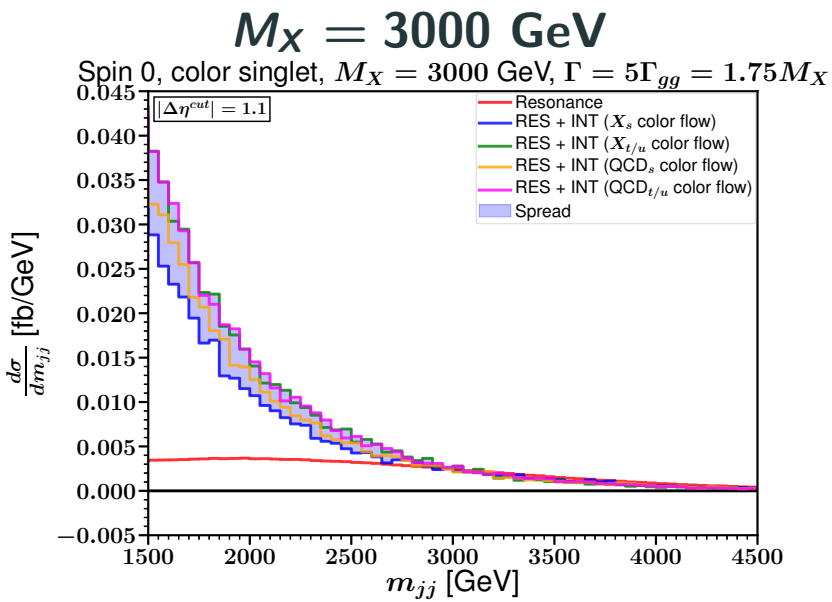

For spin-0, and spin-1 cases:

- Much larger low-mass tails compared to the case with $\Gamma = \Gamma_{gg}$.
- Dip above M_X seems to be vanishing for higher resonance masses and spins.
- Might have peak/dip or pure dip after fitting to the QCD background.

Results for $\Gamma = 5\Gamma_{gg}$: Spin 0, color octet (Monte Carlo simulations)

$M_X = 1000$ GeV

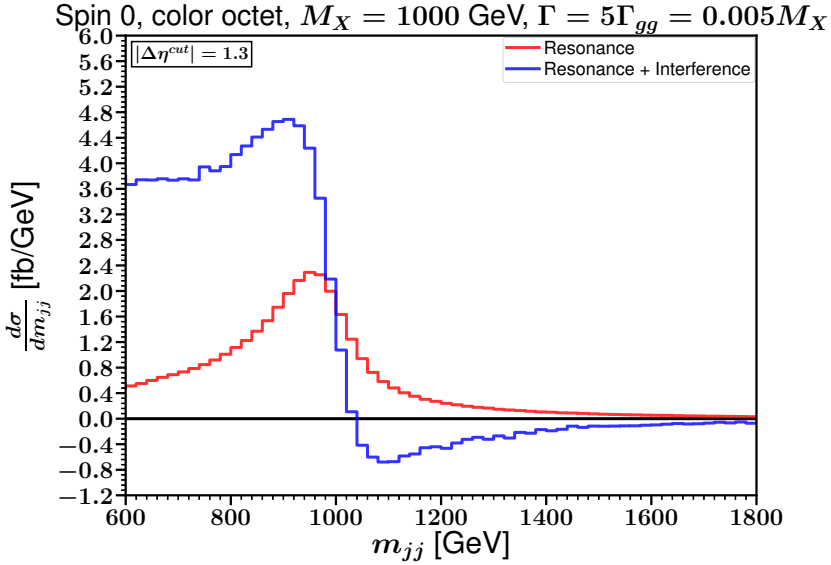

$M_X = 3000$ GeV

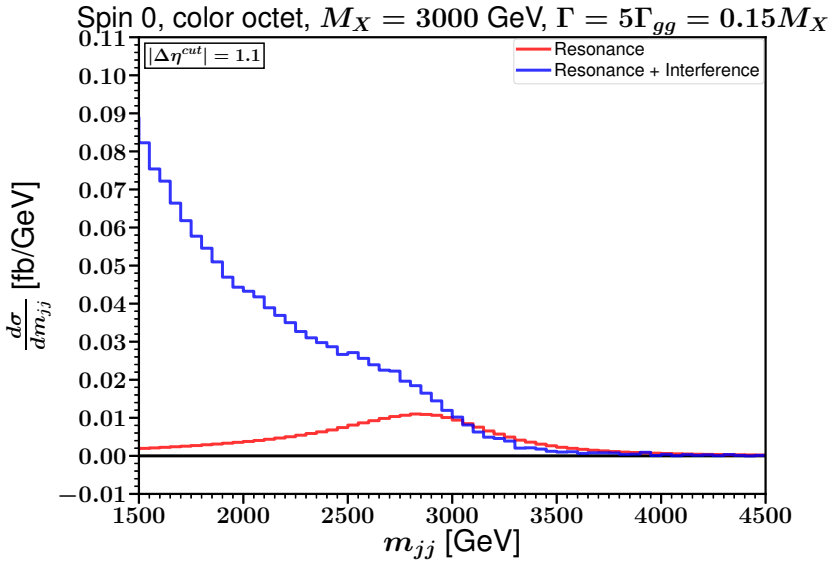

Results for $\Gamma = 5\Gamma_{gg}$: Spin 1, color octet (Monte Carlo simulations)

$M_X = 1000$ GeV

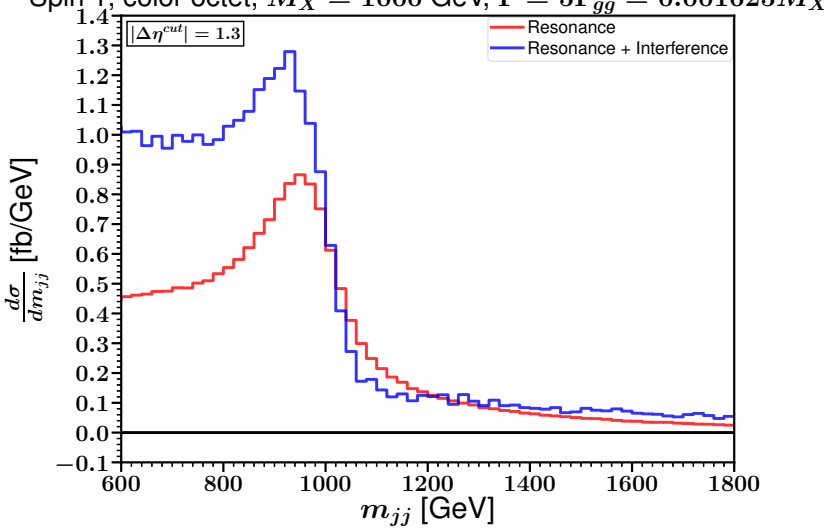

$M_X = 3000$ GeV

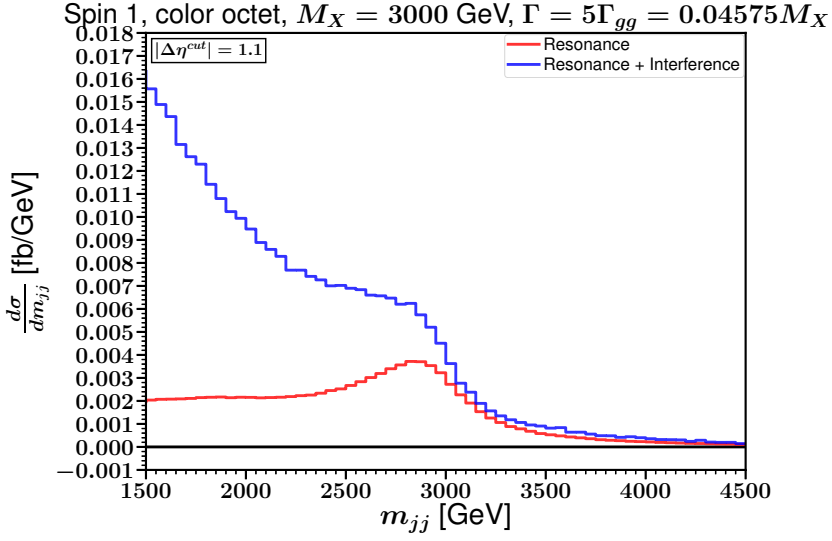

Results for $\Gamma = 5\Gamma_{gg}$: Spin 2, color singlet (Monte Carlo simulations)

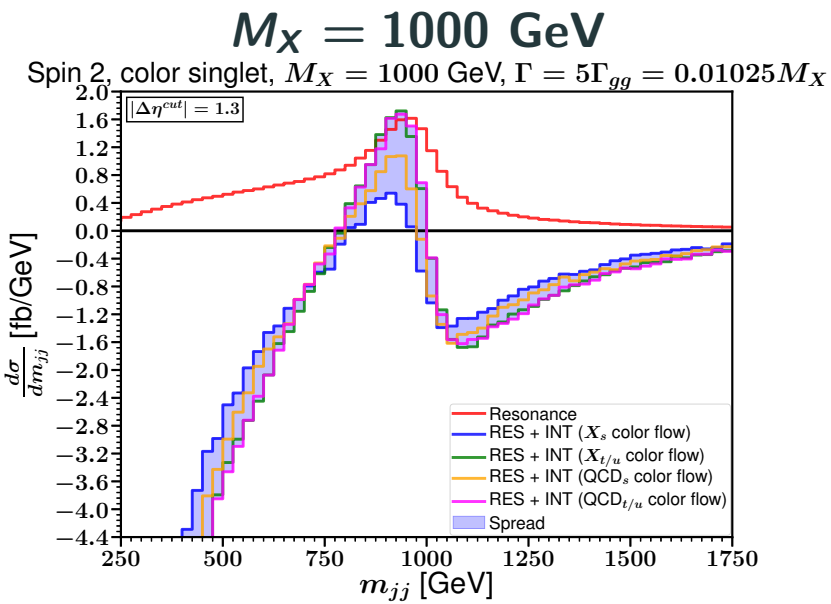

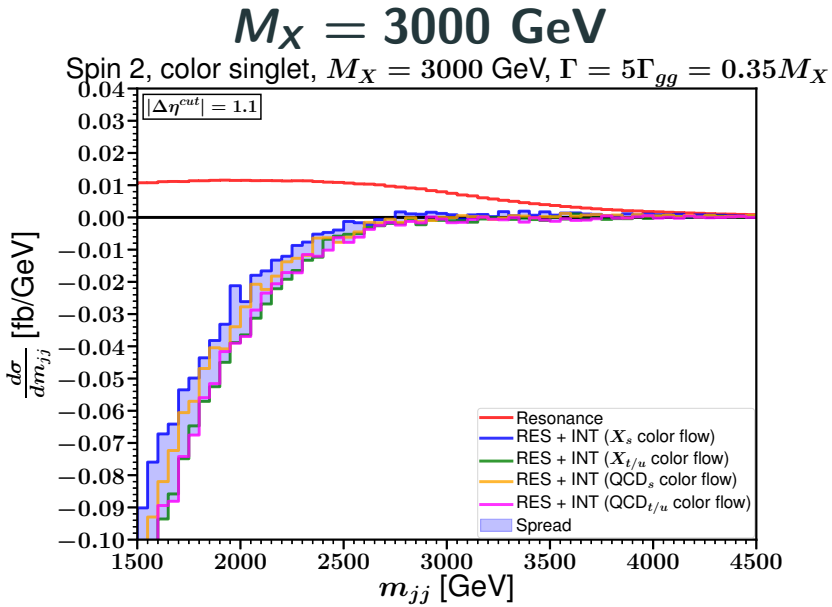

- Much larger deficit at low dijet invariant masses compared to the case with $\Gamma = \Gamma_{gg}$.
- Once again, QCD background fitting might lead to an enhanced peak much taller than naive resonance peak $\Longrightarrow$ actual limit stronger than claimed limit.

Conclusion

- Interference terms change the naive Breit-Wigner resonance peak to more like a peak-dip structure around the resonance mass.
- Particular characteristic shape depends on the spin and the color of the digluon resonance.
- Studied the interference effects (at LO) for the following digluon resonances:
  - Spin 0, color singlet
  - Spin 0, color octet
  - Spin 1, color octet
  - Spin 2, color singlet
- Considered a few benchmark examples, such that their resonant-only production cross-sections are close to the claimed exclusions of the CMS experiment in (arXiv: 1806.00843, 1911.03947).
- Interference effects larger for spin-0 color-singlet case than for spin-0 and spin-1 color-octets.
- Large (**positive**, for spin-0, spin-1; **negative**, for spin-2) low-mass tail at invariant masses well below M_X.

Conclusion (contd.)

- Low-mass tail is more significant than the high-mass deficit because the QCD background falls with $\sqrt{\hat{s}}$.
- The relative impact of the interference stays nearly constant for a fixed M_X as the resonant cross-section decreases, but tends to increase for larger M_X.
- Interference effects become more dramatic for smaller branching ratios $\mathrm{BR}(X \to gg) = \Gamma_{gg}/\Gamma$.
- After QCD background fitting and subtraction, dijet mass distributions for digluon resonances may resemble:
  - An enhanced peak
  - A shelf
  - A peak/dip
  - A pure dip
- NLO calculation with virtual 1-loop and real emission of an extra jet would provide a more realistic estimate.

THANK YOU

BACKUP SLIDES

Partonic s-channel resonant-only cross-section

The resonance partonic total cross-section (after angular integration, and with no cuts) in the narrow-width approximation is equal to

$$\hat{\sigma}(gg \to X \to gg) \quad = \quad (2j+1)k\frac{\Gamma_{gg}^2}{\Gamma M_X}\frac{\pi^2}{4}\delta(\hat{s}-M_X^2),$$

where $j = 0, 1, 2$ and $k = 1, 8$ are the spin and color of X, and $\sqrt{\hat{s}}$ is the partonic invariant mass.

> The above result reflects the fact that there are $(2j+1)k$ times more *spin* $\otimes$ *color* states for a spin j, color k resonance than for a spin-0, color-singlet.

Therefore, we chose benchmark points such that:

$$\left(\frac{\Gamma_{gg}^2}{\Gamma M_X}\right)_{\text{spin-}j,\text{color-}k} \approx \frac{1}{(2j+1)k}\left(\frac{\Gamma_{gg}^2}{\Gamma M_X}\right)_{\text{spin-0,color-singlet}},$$

in order to roughly maintain the same resonant total cross section.

Benchmark models for $M_X = 2000$ GeV[†]

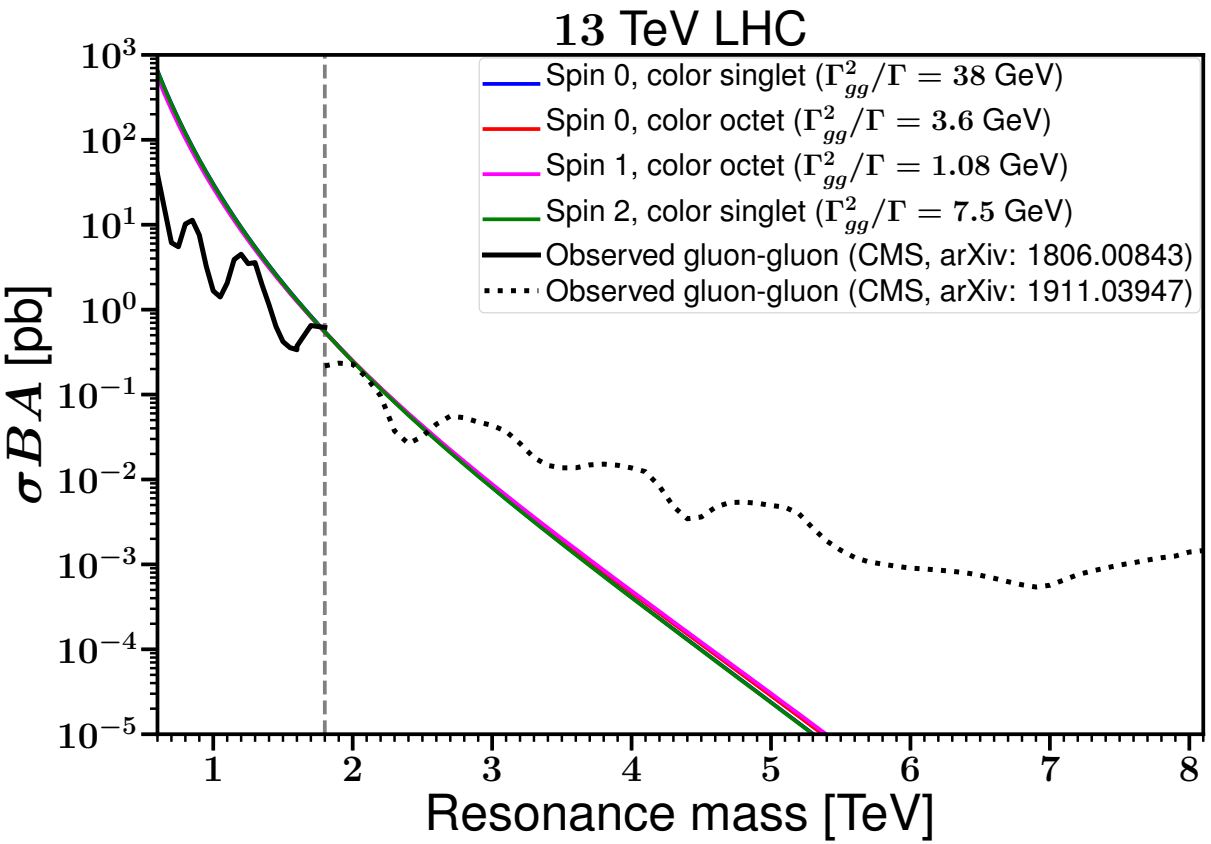

[†] For the s-channel resonant cross sections, we chose a K factor of 1.5 and an acceptance of 0.5 for the purposes of choosing the benchmarks.

(No) Landau-Yang Theorem[†]

The Landau-Yang theorem forbids:

- massive spin-1 $\rightarrow$ on-shell photon pair
- massive even-parity spin-1 $\rightarrow$ on-shell massless gauge boson pair

Does not forbid:

- massive odd-parity spin-1 $\rightarrow$ on-shell gluon pair **(our case)**
- massive spin-1 $\rightarrow$ massless gauge boson pair (if one of the three bosons is off-shell)

[†] See R. S. Chivukula, A. Farzinnia, J. Ren, E. H. Simmons 1303.1120; J. P. Ma, J. X. Wang, S. Zhao 1405.3373; W. Beenakker, R. Kleiss, G. Lustermans 1508.07115; M. Cacciari, L. Del Debbio, J. R. Espinosa, A. D. Polosa, M. Testa 1509.07853; Y. Bai, W. Y. Keung 1407.6355.

Effective Lagrangians: Spin 0, color singlet

Effective Lagrangian for a spin-0 color-singlet resonance:[†]

$$\mathcal{L} = \begin{cases} \frac{c_1}{2\Lambda} X F^a_{\mu\nu} F^{a\mu\nu} \text{ (scalar)} \\ -\frac{c_2}{4\Lambda} X \epsilon^{\mu\nu\rho\sigma} F^a_{\mu\nu} F^a_{\rho\sigma} \text{ (pseudo-scalar)} \end{cases}$$

[†] $F^a_{\mu\nu} = \partial_\mu A^a_\nu - \partial_\nu A^a_\mu - g_s f^{abc} A^b_\mu A^c_\nu$ is the QCD field strength tensor for $a, b, c = 1, 2, \ldots, 8$, and f^{abc} are the anti-symmetric structure constants of $SU(3)_c$, and g_s is the strong coupling constant.

Effective Lagrangian and Feynman rules: Spin 0, color octet

Effective Lagrangian for a spin-0 color-octet resonance:

$$\mathcal{L} = \begin{cases} \dfrac{c_3}{2\Lambda} d^{abc} X^c F^a_{\mu\nu} F^{b\mu\nu} & \text{(scalar)} \\ -\dfrac{c_4}{4\Lambda} d^{abc} X^c \epsilon^{\mu\nu\rho\sigma} F^a_{\mu\nu} F^b_{\rho\sigma} & \text{(pseudo-scalar)} \end{cases}$$

where the symmetric anomaly coefficients of $SU(3)_c$ are defined as:[†]

$$d^{abc} = 2\mathrm{Tr}[\{T^a, T^b\} T^c]$$

The corresponding Feynman rules for X-g-g coupling:

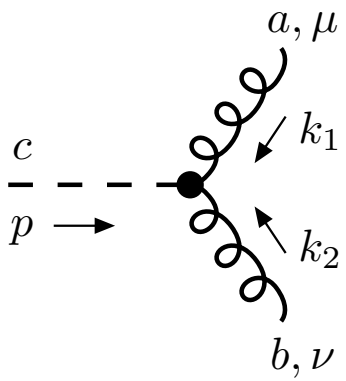

$$-i\frac{2c_3}{\Lambda} d^{abc} (k_1 \cdot k_2 \, \eta^{\mu\nu} - k_2^\mu k_1^\nu) \qquad \text{(scalar)}$$

$$-i\frac{2c_4}{\Lambda} d^{abc} \epsilon^{\mu\nu\rho\sigma} k_{1\rho} k_{2\sigma} \qquad \text{(pseudoscalar)}$$

[†] The fundamental representation matrices are normalized with the usual normalization $\mathrm{Tr}[T^a T^b] = \frac{1}{2}\delta^{ab}$, so that $d^{abc} d^{abe} = \frac{5}{3}\delta^{ce}$

Effective Lagrangian and Feynman rules: Spin 1, color octet

Effective Lagrangian for an odd-parity spin-1 color-octet resonance:[†‡]

$$\mathcal{L} \quad = \quad \frac{c_5}{\Lambda^2} f^{abc} (D_\mu X^a_\nu - D_\nu X^a_\mu) F^{b\nu\rho} F^{c\mu}_\rho ,$$

where D_μ is the gauge-covariant derivative. For X-g-g interaction $D_\mu \to \partial_\mu$.

The corresponding Feynman rule for X-g-g coupling:

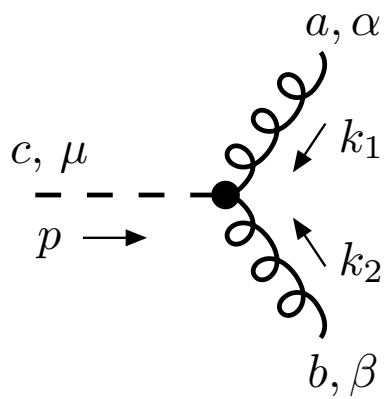

$$2i \frac{c_5}{\Lambda^2} f^{abc} (k_1 - k_2)^\mu (\eta^{\alpha\beta} k_1 \cdot k_2 - k_1^\beta k_2^\alpha)$$

[†] See M. Cacciari, L. Del Debbio, J. R. Espinosa, A. D. Polosa, M. Testa 1509.07853

[‡] As already mentioned, the Landau-Yang theorem forbids the decay of a massive even-parity spin-1 particle to two on-shell massless gauge bosons.

The Fierz-Pauli Lagrangian for a free, massive spin-2 particle

The free Lagrangian for a spin-2 resonance $X^{\mu\nu}$, with mass M_X, can be written as:[†]

$$\mathcal{L}_f = \frac{1}{2}X^{\mu\nu}\partial_\alpha\partial^\alpha X_{\mu\nu} - X^{\mu\nu}\partial_\mu\partial^\alpha X_{\nu\alpha} + X\partial_\mu\partial_\nu X^{\mu\nu} - \frac{1}{2}X\partial_\mu\partial^\mu X + \frac{1}{2}M_X^2\left[X^{\mu\nu}X_{\mu\nu} - X^2\right],$$

where $X = X^\alpha_\alpha$. The propagator for the massive spin-2 resonance is:

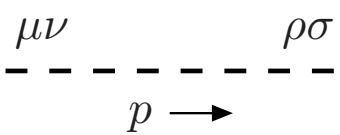

$$\frac{iD_{\mu\nu\rho\sigma}}{p^2 - M_X^2 + i\Gamma M}$$

where

$$D_{\mu\nu\rho\sigma} = \frac{1}{2}G_{\mu\rho}G_{\nu\sigma} + \frac{1}{2}G_{\mu\sigma}G_{\nu\rho} - \frac{1}{3}G_{\mu\nu}G_{\rho\sigma},$$
$$G_{\mu\nu} = \eta_{\mu\nu} - p_\mu p_\nu / M_X^2.$$

[†] See e.g. M. D. Schwartz, Quantum Field Theory and the Standard Model, Cambridge University Press, 2014

Effective Lagrangian and Feynman rules: Spin 2, color singlet

Effective Lagrangian for a spin-2 color-singlet resonance:[†]

$$\mathcal{L} = \frac{1}{\overline{M}_P} X^{\mu\nu} \left[F^a_{\mu\rho} F^{a\rho}_{\nu} - \frac{1}{4} \eta_{\mu\nu} F^a_{\rho\sigma} F^{a\rho\sigma} \right],$$

where $\overline{M}_P$ is a new mass scale.

The corresponding Feynman rule for X-g-g coupling:

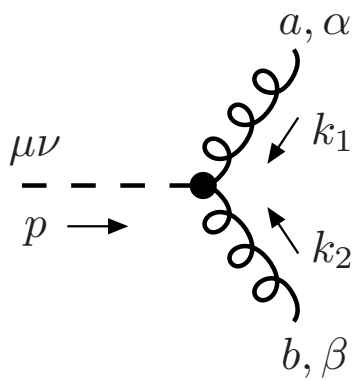

$$\frac{i}{\overline{M}_P} \delta^{ab} V^{\mu\nu\alpha\beta}$$

where

$$\begin{aligned} V^{\mu\nu\alpha\beta} = {} & k_1 \cdot k_2 (\eta^{\mu\nu}\eta^{\alpha\beta} - \eta^{\mu\alpha}\eta^{\nu\beta} - \eta^{\nu\alpha}\eta^{\mu\beta}) - \eta^{\mu\nu} k_1^\beta k_2^\alpha - (k_1^\mu k_2^\nu + k_2^\mu k_1^\nu)\eta^{\alpha\beta} \\ & + k_1^\mu k_2^\alpha \eta^{\nu\beta} + k_1^\nu k_2^\alpha \eta^{\mu\beta} + k_1^\beta k_2^\nu \eta^{\mu\alpha} + k_1^\beta k_2^\mu \eta^{\nu\alpha}. \end{aligned}$$

[†] See T. Han, J. D. Lykken, R. J. Zhang hep-ph/9811350; K. Hagiwara, J. Kanzaki, Q. Li, K. Mawatari 0805.2554 ; G. F. Giudice, R. Rattazzi, J. D. Wells hep-ph/9811291.

We can write an amplitude, for each choice of external gluon polarizations, in terms of a redundant basis of color combinations:

$$\begin{aligned}\mathcal{A}^{abcd} &= a_1 f^{abe} f^{cde} + a_2 f^{ace} f^{bde} + a_3 f^{ade} f^{bce} \\ &\quad + a_4 \delta^{ab} \delta^{cd} + a_5 \delta^{ac} \delta^{bd} + a_6 \delta^{ad} \delta^{bc} \\ &\quad + a_7 d^{abe} d^{cde} + a_8 d^{ace} d^{bde} + a_9 d^{ade} d^{bce}.\end{aligned}$$

which then leads to the color sum:

$$\begin{aligned}\sum_{a,b,c,d} |\mathcal{A}^{abcd}|^2 &= 72 \left(|a_1|^2 + |a_2|^2 + |a_3|^2 \right) + 72 \,\mathrm{Re}[a_1 a_2^* - a_1 a_3^* + a_2 a_3^*] \\ &\quad + 64 \left(|a_4|^2 + |a_5|^2 + |a_6|^2 \right) + 16 \,\mathrm{Re}[a_4 a_5^* + a_4 a_6^* + a_5 a_6^*] \\ &\quad + \frac{200}{9} \left(|a_7|^2 + |a_8|^2 + |a_9|^2 \right) - \frac{40}{3} \,\mathrm{Re}[a_7 a_8^* + a_7 a_9^* + a_8 a_9^*] \\ &\quad + 48 \,\mathrm{Re}[a_1 a_5^* - a_1 a_6^* + a_2 a_4^* - a_2 a_6^* + a_3 a_4^* - a_3 a_5^*] \\ &\quad + 40 \,\mathrm{Re}[a_1 a_8^* - a_1 a_9^* + a_2 a_7^* - a_2 a_9^* + a_3 a_7^* - a_3 a_8^*] \\ &\quad + \frac{80}{3} \,\mathrm{Re}[a_4 a_8^* + a_4 a_9^* + a_5 a_7^* + a_5 a_9^* + a_6 a_7^* + a_6 a_8^*].\end{aligned}$$

Redundancy in the amplitude $\mathcal{A}^{abcd}$

Only five of the nine a_is are independent, because of the following QCD identities[†]:

$$f^{abe}f^{cde} + f^{ace}f^{dbe} + f^{ade}f^{bce} = 0, \quad (1)$$

$$d^{abe}d^{cde} - \frac{1}{3}\left(f^{ace}f^{bde} + f^{ade}f^{bce}\right) = \frac{1}{3}\left(\delta^{ac}\delta^{bd} + \delta^{ad}\delta^{bc} - \delta^{ab}\delta^{cd}\right), \quad (2)$$

$$f^{abe}f^{cde} - d^{ace}d^{bde} + d^{bce}d^{ade} = \frac{2}{N_c}\left(\delta^{ac}\delta^{bd} - \delta^{ad}\delta^{bc}\right), \quad (3)$$

$$d^{abe}d^{cde} + d^{ace}d^{bde} + d^{ade}d^{bce} = \frac{1}{3}\left(\delta^{ab}\delta^{cd} + \delta^{ac}\delta^{bd} + \delta^{ad}\delta^{bc}\right). \quad (4)$$

Some comments:

- Eq. (1) & eq. (3) hold true for $SU(N_c)$. Eq. (2) & eq. (4) are special to $SU(3)$.
- The above 4 eqs. are not independent of each other. Namely, eq. (3) & eq. (4) $\rightarrow$ eq. (2); eq. (2) & eq. (3) $\rightarrow$ eq. (1) & eq. (4).
- Using eqs. (1) & (2), we can eliminate a_7, a_8, a_9, & one of a_1, a_2, or a_3.
- Or we can use eqs. (3) & (4) to eliminate a_1, a_2, a_3, & one of a_7, a_8, or a_9.
- In any case, can eliminate 4 out of 9 a_is.

[†] See e.g. H. E. Haber 1912.13302; A. J. MacFarlane, A. Sudbery, P. H. Weisz doi:10.1007/BF01654302 (1968).

QCD and resonant amplitudes (contd.)

There are natural choices for a_i (in $\mathcal{A}^{abcd}$) that follow from the Feynman rules.

After including the contributions from t- and u-channel exchanges of X, and the interferences with QCD amplitudes:

$$a_7 = a_8 = a_9 = 0 \quad \text{(color-singlets)}$$
$$a_4 = a_5 = a_6 = 0 \quad \text{(spin-0 color-octet)}$$
$$a_4 = a_5 = a_6 = a_7 = a_8 = a_9 = 0 \quad \text{(spin-1 color-octet)}$$

$\sum_{a,b,c,d} |\mathcal{A}^{abcd}|^2$ is then summed over all the final states, averaged over all the initial states for both color and spin to obtain the complete LO partonic differential cross-section of:

- X exchange diagrams (resonant signal)
- Pure QCD background
- The interference between the signal and the background processes

Analytic formulas - Spin 0, color singlet

The resonant and interference partonic cross sections at LO for both parity-even and parity-odd spin 0, color singlets (i.e. $i = 1, 2$) are:

$$\begin{aligned}
\frac{d\hat{\sigma}_{\mathrm{s}}}{dz} &= \frac{|c_i|^4 \hat{s}^3}{32\pi\Lambda^4 D(\hat{s})}, \\
\frac{d\hat{\sigma}_{\mathrm{t}}}{dz} + \frac{d\hat{\sigma}_{\mathrm{u}}}{dz} &= \frac{|c_i|^4}{32\pi\Lambda^4 \hat{s}} \left[\frac{\hat{t}^4}{D(\hat{t})} + \frac{\hat{u}^4}{D(\hat{u})} \right], \\
\frac{d\hat{\sigma}_{\mathrm{s,t}}}{dz} &= \frac{|c_i|^4 \hat{s}\hat{t}^2}{256\pi\Lambda^4 D(\hat{s})D(\hat{t})} \left[(\hat{s} - M_X^2)(\hat{t} - M_X^2) + \Gamma^2 M_X^2 \right], \\
\frac{d\hat{\sigma}_{\mathrm{t,u}}}{dz} &= \frac{|c_i|^4 \hat{t}^2\hat{u}^2}{256\pi\Lambda^4 \hat{s} D(\hat{t})D(\hat{u})} \left[(\hat{t} - M_X^2)(\hat{u} - M_X^2) + \Gamma^2 M_X^2 \right], \\
\frac{d\hat{\sigma}_{\mathrm{s,u}}}{dz} &= \frac{|c_i|^4 \hat{s}\hat{u}^2}{256\pi\Lambda^4 D(\hat{s})D(\hat{u})} \left[(\hat{s} - M_X^2)(\hat{u} - M_X^2) + \Gamma^2 M_X^2 \right], \\
\frac{d\hat{\sigma}_{\mathrm{s,QCD}}}{dz} &= -\frac{3\alpha_S \hat{s}}{8\Lambda^2 D(\hat{s})(1 - z^2)} \left\{ \mathrm{Re}[c_i^2](\hat{s} - M_X^2) + \mathrm{Im}[c_i^2]\Gamma M_X \right\}, \\
\frac{d\hat{\sigma}_{\mathrm{t,QCD}}}{dz} &= \frac{3\alpha_S \hat{s}(1 - z)^4}{256\Lambda^2 D(\hat{t})(1 + z)} \left\{ \mathrm{Re}[c_i^2](\hat{t} - M_X^2) + \mathrm{Im}[c_i^2]\Gamma M_X \right\}, \\
\frac{d\hat{\sigma}_{\mathrm{u,QCD}}}{dz} &= \frac{3\alpha_S \hat{s}(1 + z)^4}{256\Lambda^2 D(\hat{u})(1 - z)} \left\{ \mathrm{Re}[c_i^2](\hat{u} - M_X^2) + \mathrm{Im}[c_i^2]\Gamma M_X \right\},
\end{aligned}$$

where $\hat{t} = \hat{s}(z - 1)/2$ and $\hat{u} = -\hat{s}(z + 1)/2$, and

$$\begin{aligned}
D(\hat{s}) &\equiv (\hat{s} - M_X^2)^2 + \Gamma^2 M_X^2. \\
\Gamma_{gg} &= \frac{|c_i|^2 M_X^3}{2\pi\Lambda^2} \text{ (LO digluon partial width)}
\end{aligned}$$

Analytic formulas - Spin 0, color octet

The resonant and interference partonic cross sections at LO for both scalar and pseudo-scalar color octets (i.e. $i = 3, 4$) are:

$$
\begin{aligned}
\frac{d\hat{\sigma}_{\mathrm{s}}}{dz} &= \frac{25|c_i|^4\hat{s}^3}{2304\pi\Lambda^4 D(\hat{s})}, \\
\frac{d\hat{\sigma}_{\mathrm{t}}}{dz} + \frac{d\hat{\sigma}_{\mathrm{u}}}{dz} &= \frac{25|c_i|^4}{2304\pi\Lambda^4\hat{s}}\left[\frac{\hat{t}^4}{D(\hat{t})} + \frac{\hat{u}^4}{D(\hat{u})}\right], \\
\frac{d\hat{\sigma}_{\mathrm{s,t}}}{dz} &= -\frac{5|c_i|^4\hat{s}\hat{t}^2}{1536\pi\Lambda^4 D(\hat{s})D(\hat{t})}\left[(\hat{s}-M_X^2)(\hat{t}-M_X^2)+\Gamma^2M_X^2\right], \\
\frac{d\hat{\sigma}_{\mathrm{t,u}}}{dz} &= -\frac{5|c_i|^4\hat{t}^2\hat{u}^2}{1536\pi\Lambda^4\hat{s}D(\hat{t})D(\hat{u})}\left[(\hat{t}-M_X^2)(\hat{u}-M_X^2)+\Gamma^2M_X^2\right], \\
\frac{d\hat{\sigma}_{\mathrm{s,u}}}{dz} &= -\frac{5|c_i|^4\hat{s}\hat{u}^2}{1536\pi\Lambda^4 D(\hat{s})D(\hat{u})}\left[(\hat{s}-M_X^2)(\hat{u}-M_X^2)+\Gamma^2M_X^2\right], \\
\frac{d\hat{\sigma}_{\mathrm{s,QCD}}}{dz} &= -\frac{5\alpha_S\hat{s}}{16\Lambda^2 D(\hat{s})(1-z^2)}\left\{\mathrm{Re}[c_i^2](\hat{s}-M_X^2)+\mathrm{Im}[c_i^2]\Gamma M_X\right\}, \\
\frac{d\hat{\sigma}_{\mathrm{t,QCD}}}{dz} &= \frac{5\alpha_S\hat{s}(1-z)^4}{512\Lambda^2 D(\hat{t})(1+z)}\left\{\mathrm{Re}[c_i^2](\hat{t}-M_X^2)+\mathrm{Im}[c_i^2]\Gamma M_X\right\}, \\
\frac{d\hat{\sigma}_{\mathrm{u,QCD}}}{dz} &= \frac{5\alpha_S\hat{s}(1+z)^4}{512\Lambda^2 D(\hat{u})(1-z)}\left\{\mathrm{Re}[c_i^2](\hat{u}-M_X^2)+\mathrm{Im}[c_i^2]\Gamma M_X\right\},
\end{aligned}
$$

and the partial width into the digluon final state is

$$
\Gamma_{gg} = \frac{5|c_i|^2 M_X^3}{48\pi\Lambda^2}.
$$

Analytic formulas - Spin 1, color octet

The resonant and interference partonic cross sections at LO for a spin-1, color-octet resonance are:

$$
\begin{aligned}
\frac{d\hat{\sigma}_{\mathrm{s}}}{dz} &= \frac{9|c_5|^4\hat{s}^5 z^2}{256\pi\Lambda^8 D(\hat{s})}, \\
\frac{d\hat{\sigma}_{\mathrm{t}}}{dz} + \frac{d\hat{\sigma}_{\mathrm{u}}}{dz} &= \frac{9|c_5|^4\hat{s}}{1024\pi\Lambda^8}\left[\frac{\hat{t}^4(3+z)^2}{D(\hat{t})} + \frac{\hat{u}^4(3-z)^2}{D(\hat{u})}\right], \\
\frac{d\hat{\sigma}_{\mathrm{s,t}}}{dz} &= \frac{9|c_5|^4\hat{s}^3\hat{t}^2 z(3+z)}{1024\pi\Lambda^8 D(\hat{s})D(\hat{t})}\left[(\hat{s}-M_X^2)(\hat{t}-M_X^2)+\Gamma^2 M_X^2\right], \\
\frac{d\hat{\sigma}_{\mathrm{t,u}}}{dz} &= \frac{9|c_5|^4\hat{s}\hat{t}^2\hat{u}^2(9-z^2)}{2048\pi\Lambda^8 D(\hat{t})D(\hat{u})}\left[(\hat{t}-M_X^2)(\hat{u}-M_X^2)+\Gamma^2 M_X^2\right], \\
\frac{d\hat{\sigma}_{\mathrm{s,u}}}{dz} &= -\frac{9|c_5|^4\hat{s}^3\hat{u}^2 z(3-z)}{1024\pi\Lambda^8 D(\hat{s})D(\hat{u})}\left[(\hat{s}-M_X^2)(\hat{u}-M_X^2)+\Gamma^2 M_X^2\right], \\
\frac{d\hat{\sigma}_{\mathrm{s,QCD}}}{dz} &= -\frac{9\alpha_S\hat{s}^2 z^2}{16\Lambda^4 D(\hat{s})(1-z^2)}\left\{\mathrm{Re}[c_5^2](\hat{s}-M_X^2)+\mathrm{Im}[c_5^2]\Gamma M_X\right\}, \\
\frac{d\hat{\sigma}_{\mathrm{t,QCD}}}{dz} &= -\frac{9\alpha_S\hat{s}^2(3+z)^2(1-z)^3}{1024\Lambda^4 D(\hat{t})(1+z)}\left\{\mathrm{Re}[c_5^2](\hat{t}-M_X^2)+\mathrm{Im}[c_5^2]\Gamma M_X\right\}, \\
\frac{d\hat{\sigma}_{\mathrm{u,QCD}}}{dz} &= -\frac{9\alpha_S\hat{s}^2(3-z)^2(1+z)^3}{1024\Lambda^4 D(\hat{u})(1-z)}\left\{\mathrm{Re}[c_5^2](\hat{u}-M_X^2)+\mathrm{Im}[c_5^2]\Gamma M_X\right\},
\end{aligned}
$$

and the partial width into the digluon final state is

$$
\Gamma_{gg} = \frac{|c_5|^2 M_X^5}{16\pi\Lambda^4}.
$$

Analytic formulas - Spin 2, color singlet

The resonant and interference partonic cross sections at LO for a spin-2, color-singlet resonance are:

$$
\begin{aligned}
\frac{d\hat{\sigma}_{\mathrm{s}}}{dz} &= \frac{\hat{s}^3(1+6z^2+z^4)}{512\pi\overline{M}_P^4 D(\hat{s})}, \\
\frac{d\hat{\sigma}_{\mathrm{t}}}{dz}+\frac{d\hat{\sigma}_{\mathrm{u}}}{dz} &= \frac{\hat{s}^3}{1024\pi\overline{M}_P^4}\left[\frac{(17+4z+6z^2+4z^3+z^4)}{D(\hat{t})}+\frac{(17-4z+6z^2-4z^3+z^4)}{D(\hat{u})}\right], \\
\frac{d\hat{\sigma}_{\mathrm{s,t}}}{dz} &= \frac{\hat{s}^3(1+z)^4}{4096\pi\overline{M}_P^4 D(\hat{s})D(\hat{t})}\left[(\hat{s}-M_X^2)(\hat{t}-M_X^2)+\Gamma^2 M_X^2\right], \\
\frac{d\hat{\sigma}_{\mathrm{t,u}}}{dz} &= \frac{\hat{s}^3}{256\pi\overline{M}_P^4 D(\hat{t})D(\hat{u})}\left[(\hat{t}-M_X^2)(\hat{u}-M_X^2)+\Gamma^2 M_X^2\right], \\
\frac{d\hat{\sigma}_{\mathrm{s,u}}}{dz} &= \frac{\hat{s}^3(1-z)^4}{4096\pi\overline{M}_P^4 D(\hat{s})D(\hat{u})}\left[(\hat{s}-M_X^2)(\hat{u}-M_X^2)+\Gamma^2 M_X^2\right], \\
\frac{d\hat{\sigma}_{\mathrm{s,QCD}}}{dz} &= -\frac{3\alpha_S\hat{s}(\hat{s}-M_X^2)(1+6z^2+z^4)}{64\overline{M}_P^2 D(\hat{s})(1-z^2)}, \\
\frac{d\hat{\sigma}_{\mathrm{t,QCD}}}{dz} &= \frac{3\alpha_S\hat{s}(\hat{t}-M_X^2)(17+4z+6z^2+4z^3+z^4)}{256\overline{M}_P^2 D(\hat{t})(1-z^2)}, \\
\frac{d\hat{\sigma}_{\mathrm{u,QCD}}}{dz} &= \frac{3\alpha_S\hat{s}(\hat{u}-M_X^2)(17-4z+6z^2-4z^3+z^4)}{256\overline{M}_P^2 D(\hat{u})(1-z^2)}.
\end{aligned}
$$

The digluon partial width of the resonance is

$$
\Gamma_{gg} = \frac{M_X^3}{10\pi\overline{M}_P^2}.
$$

Kinematic cuts for parton-level approximation

Object cuts:

$$\begin{aligned} p_{T_j} > p_{T_j}^{\rm cut} &= 100 \text{ GeV}, \\ |\eta_j| < \eta_j^{\rm cut} &= 2.5. \end{aligned}$$

To increase the significance of resonant signal:

$$\Delta\eta = |\eta_{j_1} - \eta_{j_2}| < (\Delta\eta)^{\rm cut} = \begin{cases} 1.3 \text{ (for } M_X < 1800 \text{ GeV, CMS 1806.00843)} \\ 1.1 \text{ (for } M_X > 1800 \text{ GeV, CMS 1911.03947)} \end{cases}$$

For parton-level analysis, we impose these cuts by choosing:

$$\begin{aligned} x_\pm &= e^{\pm\eta_j^{\rm cut}} \sqrt{\hat{s}/s}, \\ z_{\rm cut} &= \text{Min}\left[\sqrt{1 - 4p_{T_j}^{\rm cut\,2}/\hat{s}},\ \tanh\left(\eta_j^{\rm cut} - \frac{1}{2}\left|\ln\left(x^2 s/\hat{s}\right)\right|\right),\ \tanh\left((\Delta\eta)^{\rm cut}/2\right)\right] \end{aligned}$$

while computing $d\sigma_{pp\to gg}/dm_{gg}$.

Parton-level approximation

To obtain more realistic distributions

> The parton-level distributions of $d\sigma_{pp\to gg}/d(\sqrt{\hat{s}})$ [see slide 7, 43] are smeared by convolution with an approximate detector response dijet mass distribution (shown in slide 45).

This method can be viewed as a quick approximation and qualitative independent cross-check of the results obtained using Monte Carlo event generators.

Approximate detector responses

The normalized detector response dijet mass distributions for two possibly "wide jets"[†], for each of the four (spin, color) combinations.

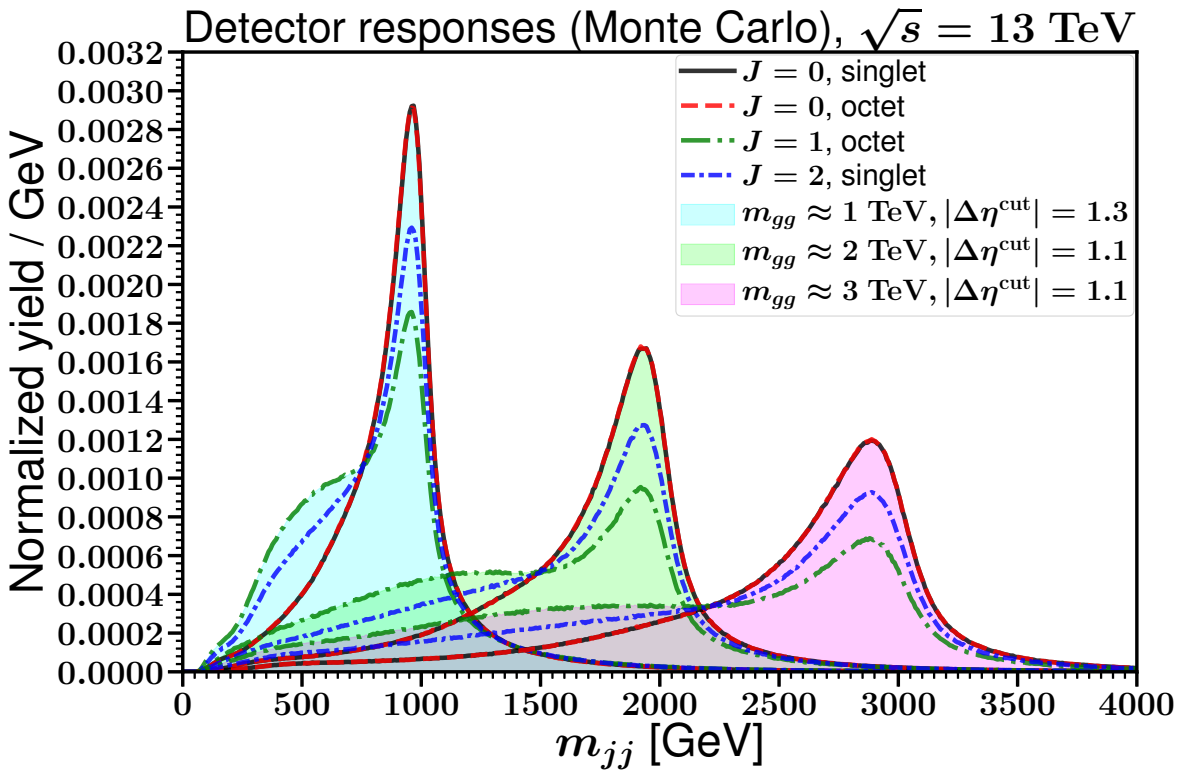

Obtained using PYTHIA 8.2 and DELPHES 3.4, from ($\geq$ 15 million) parton-level events with $\sqrt{\hat{s}} = m_{gg} = M_X = (1000, 2000, 3000)$ GeV.

[†] Wide jets are defined in Slide 8

Results for $\Gamma = \Gamma_{gg}$: Spin 0, color singlet (parton-level approximation)

$M_X = 1000$ GeV:

Partonic

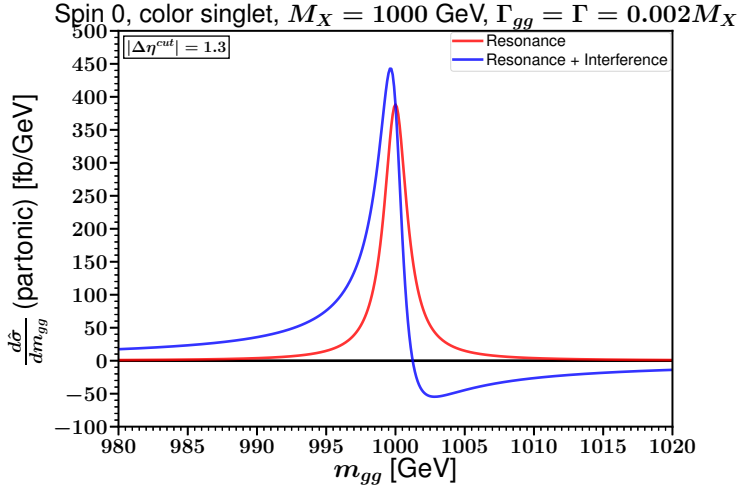

Smeared partonic

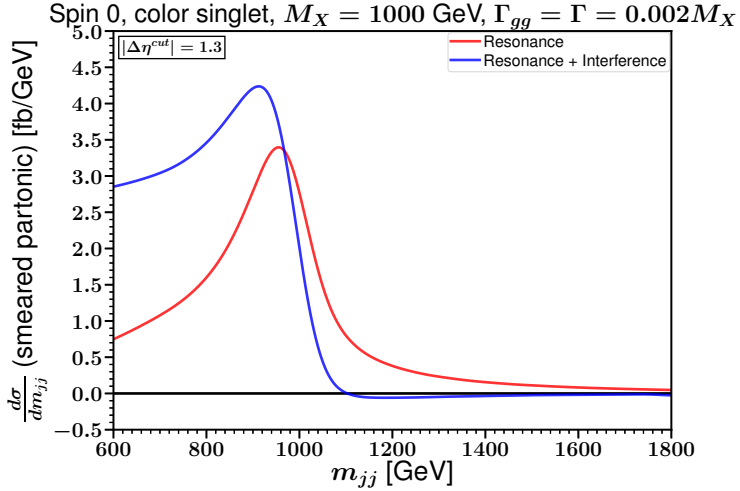

$M_X = 3000$ GeV:

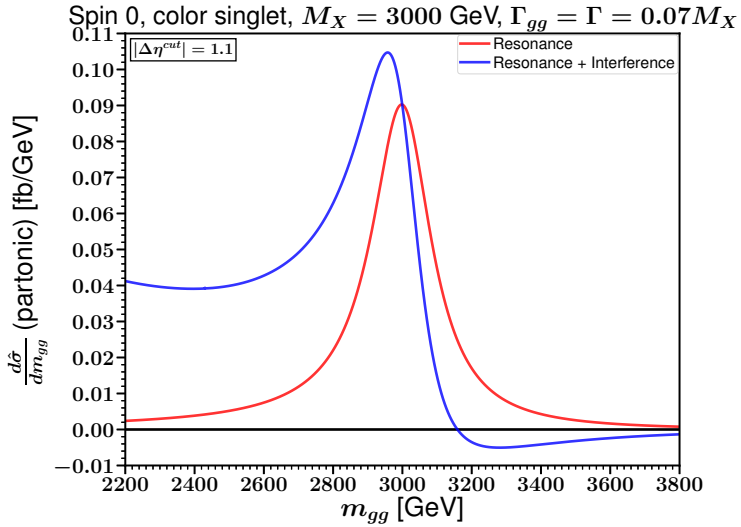

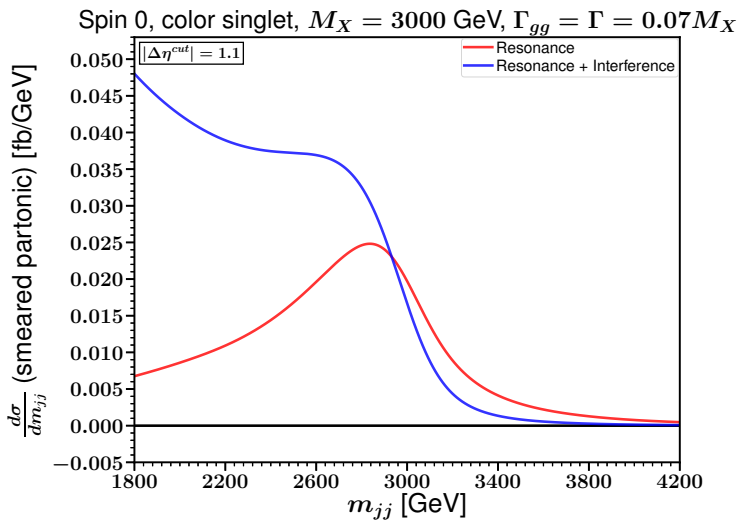

Discussions for $\Gamma = \Gamma_{gg}$: Spin 0, color singlet

- The full results are both qualitatively and quantitatively different from that of naive resonance peak.
- In the parton-level results, we see a peak/dip signature, which can be traced back to the term $\hat{s} - M_X^2$ in $d\hat{\sigma}_{\mathrm{s,QCD}}/dz$ [see Slide 39]. After smearing (and in the simulation results), the dip at higher invariant masses manifests as a deficit of events compared to the naive resonance results, and there is a large low-energy tail.
- The magnitude of the interference is, in general, enhanced for $\sqrt{\hat{s}}$ below M_X because of the steeply falling gluon PDFs.
- If the low-energy tail is absorbed into a QCD background fit (which we do not attempt here), an effective dip for $m_{jj} > M_X$ would probably result.
- The relative importance of interference seems to increase with the resonance mass.
- The plots obtained by parton-level approximation can be compared to the ones obtained by full event simulation method.[†]

[†] The match is of course not an exact one, because the smearing method using the detector responses in Slide 45, is only a very rough approximation to the full-fledged event generation with showering, hadronization and detector simulation, and furthermore the color-flow uncertainty is evidently a non-trivial one.

Results for $\Gamma = \Gamma_{gg}$: Spin 0, color octet (parton-level approximation)

$M_X = 1000$ GeV:

Partonic

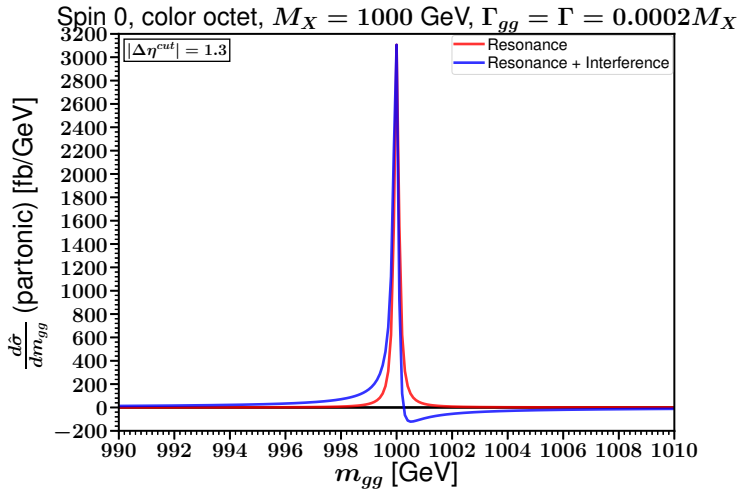

Smeared partonic

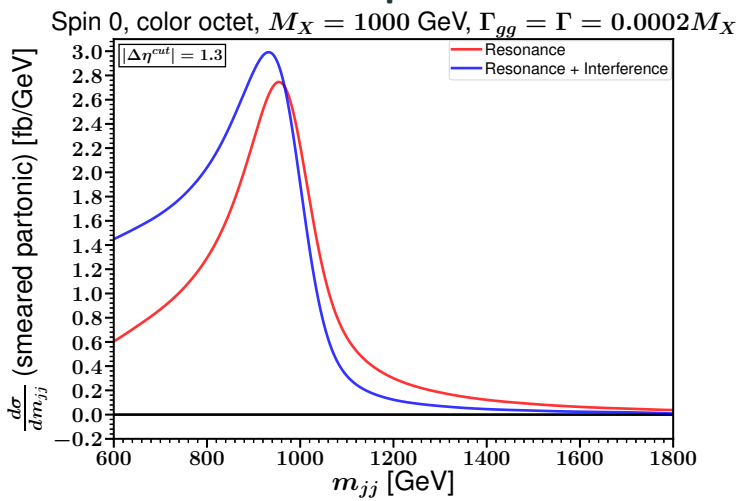

$M_X = 3000$ GeV:

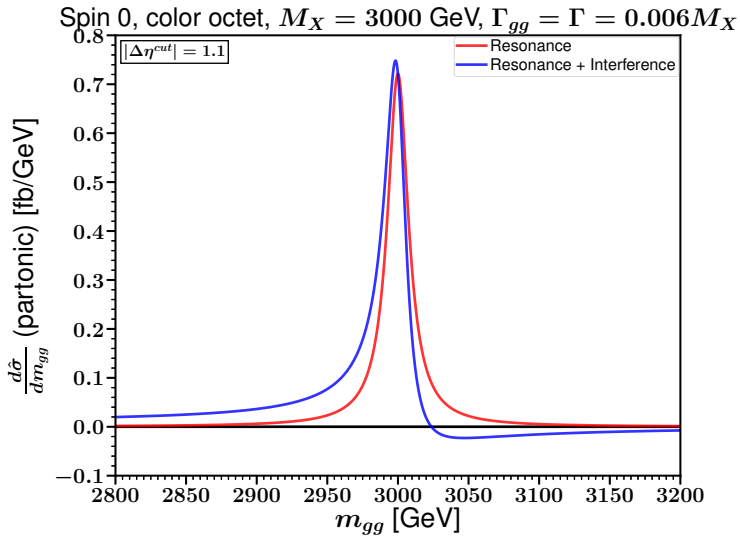

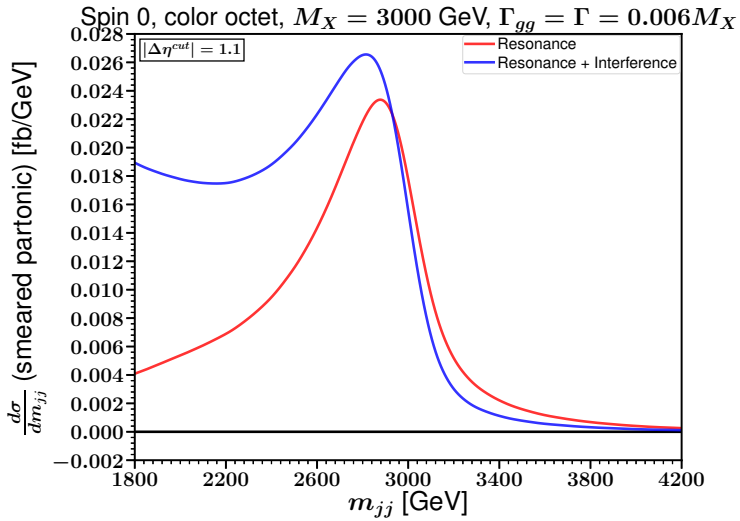

Discussions for $\Gamma = \Gamma_{gg}$: Spin 0, color octet

- There is, again, a peak/dip signature at $m_{gg} \approx M_X$ in the parton-level results. After smearing (and in the simulation results), the main feature is again the presence of the low-mass positive tail.
- Depending on how the low-mass tail would be absorbed into the QCD background fit, this could again lead to both a peak slightly below M_X and an apparent dip in the differential distribution above M_X.
- The relative importance of interference seems to increase with the resonance mass.
- The interference effects for spin-0, color-octet resonances are not as big as for spin-0, color-singlets.

Results for $\Gamma = \Gamma_{gg}$: Spin 1, color octet (parton-level approximation)

$M_X = 1000$ GeV:

Partonic

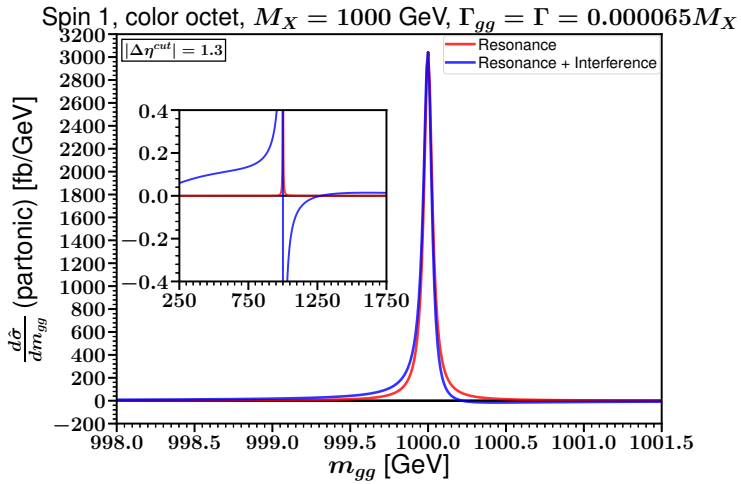

Smeared partonic

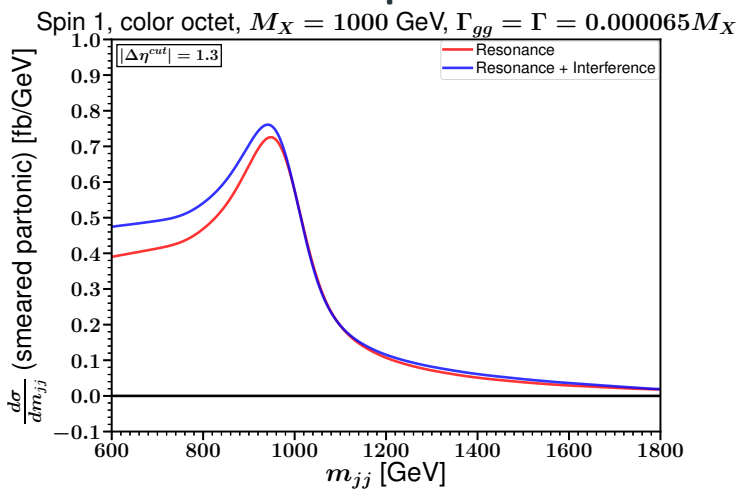

$M_X = 3000$ GeV:

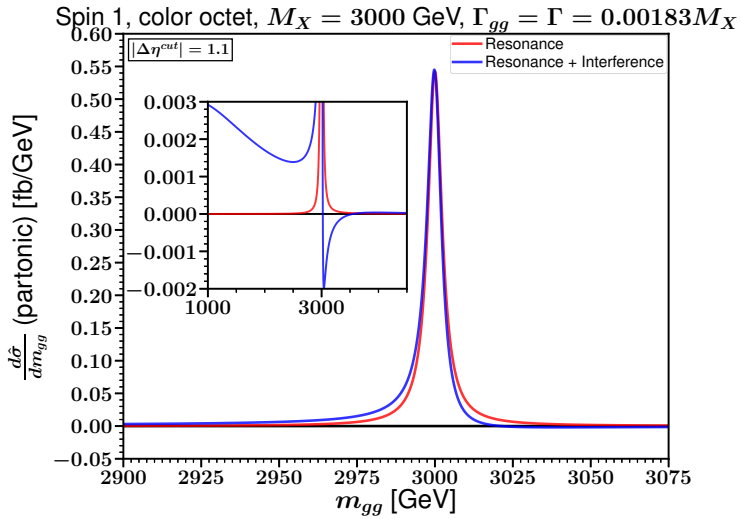

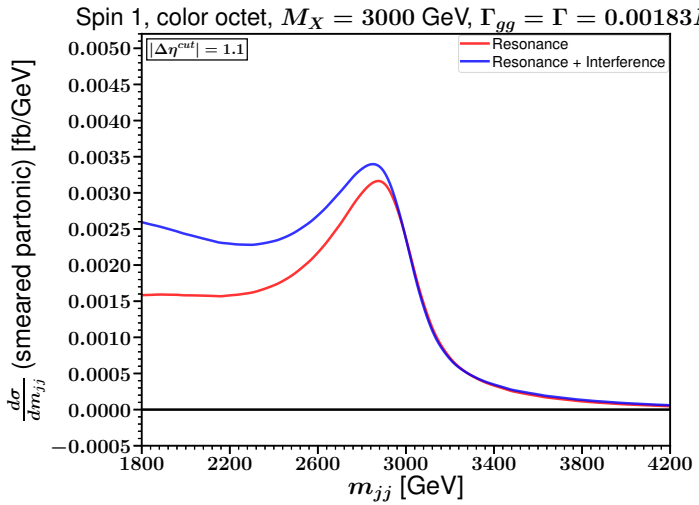

Discussions for $\Gamma = \Gamma_{gg}$: Spin 1, color octet

- The results with QCD interferences has peak below M_X, which is almost comparable to the pure peak (without QCD interferences).
- The differential cross sections in the region $m_{jj} > M_X$ are almost unaffected by including the interference.
- However, as before, the presence of the large low-mass tail means that after fitting the QCD background, the residual distribution may have an apparent dip above M_X.
- The relative importance of interference seems to increase with the resonance mass.
- In this case, the difference between the shapes found with the parton-level smearing method and the full event simulation method is more significant than in the spin-0 case, this time with a larger yield and a more pronounced low-mass tail using the latter, presumably more accurate, method.

Results for $\Gamma = \Gamma_{gg}$: Spin 2, color singlet (parton-level approximation)

$M_X = 1000$ GeV:

Partonic

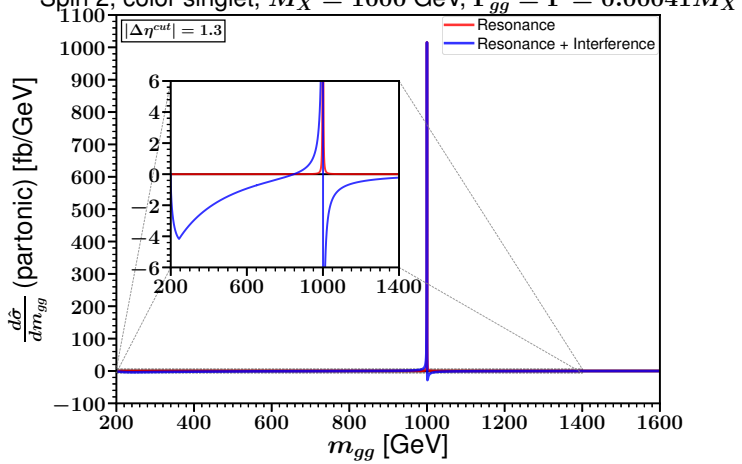

Smeared partonic

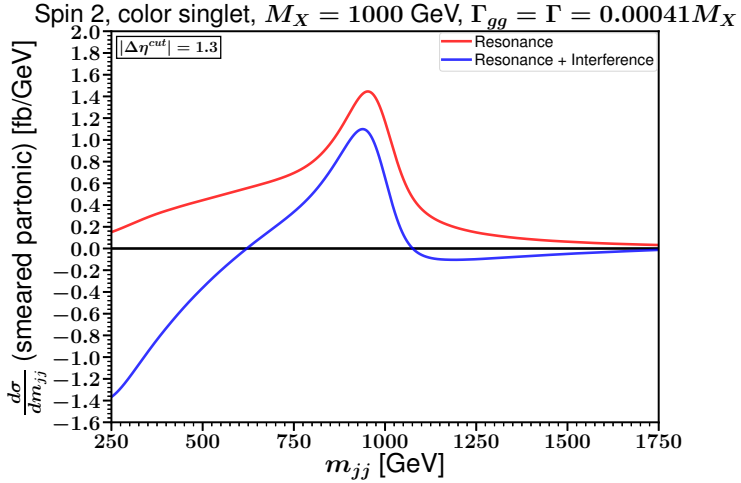

$M_X = 3000$ GeV:

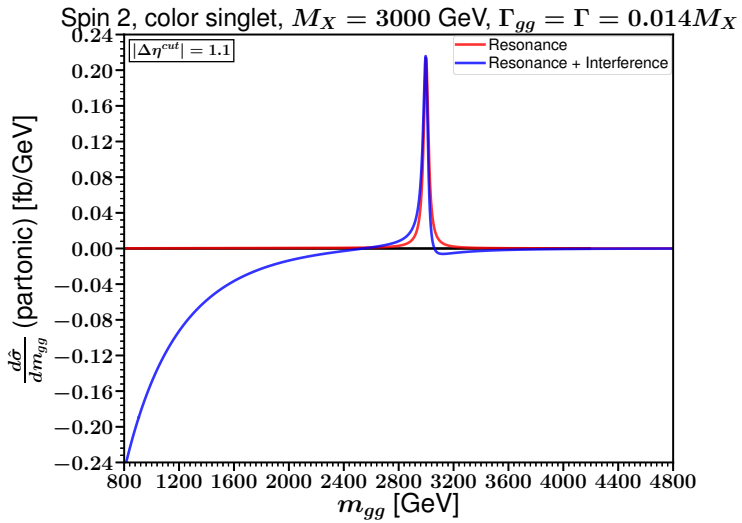

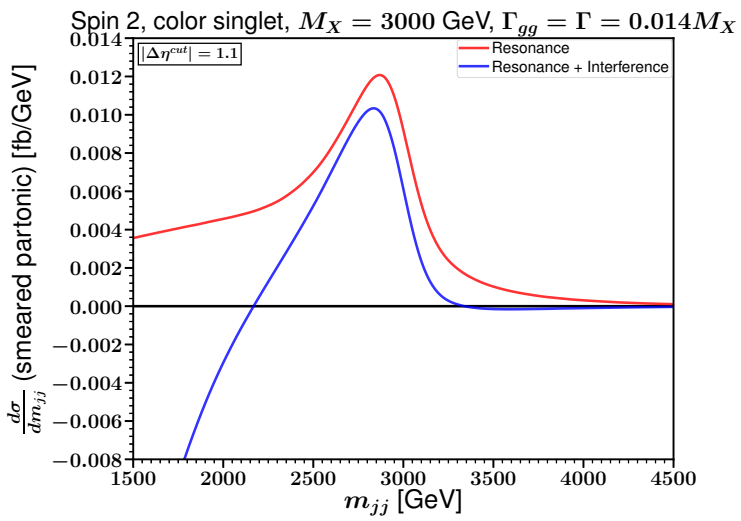

A closer look at spin 2, color singlet (parton-level)

The negative tails at small invariant mass come from the interference between the QCD amplitudes and the t- and u-channel X exchange diagrams:

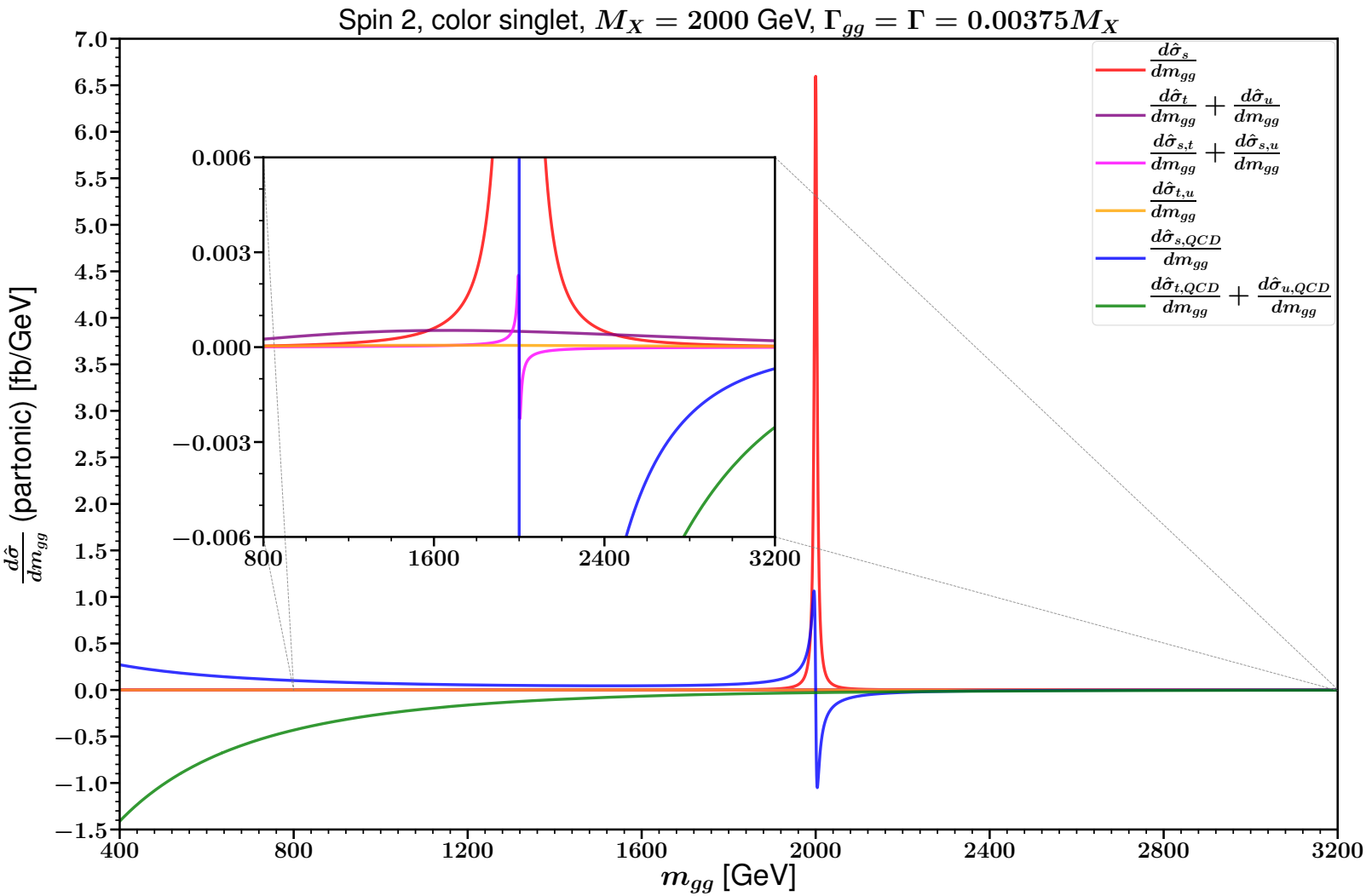

Discussions for $\Gamma = \Gamma_{gg}$: Spin 2, color singlet

- The effect of the interference is negative (in both parton- and detector-level plots) for invariant masses well below M_X, due to contributions from the interference between t-, and u-channel X exchange diagrams and the QCD diagrams (A feature unique to this case).
- Then, similar to the case of spin-0 color-singlet resonances, there is a peak/dip pattern around the resonance mass $m_{jj} \approx M_X$.
- The net effect of negative interference both above and below the M_X means that, after fitting to the QCD background, the resonance peak could actually stand out more prominently than predicted by the naive pure-resonance prediction.
- The relative importance of interference seems to increase with the resonance mass.

Results for $\Gamma = 5\Gamma_{gg}$: Spin 0, color singlet (parton-level approximation)

$M_X = 1000$ GeV:

Partonic

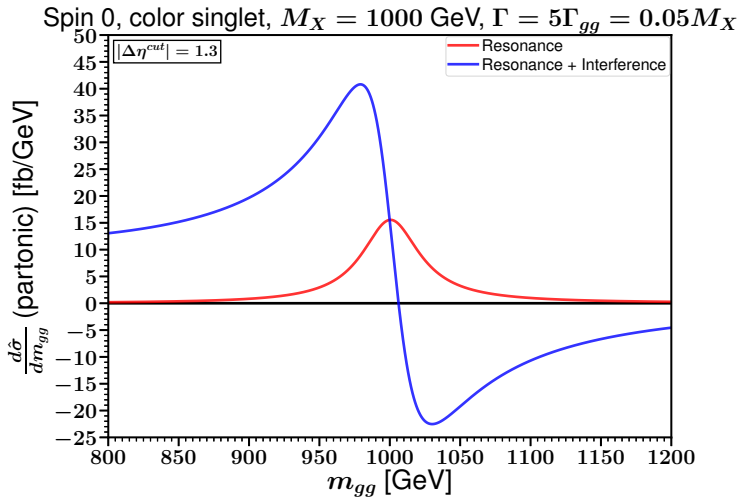

Smeared partonic

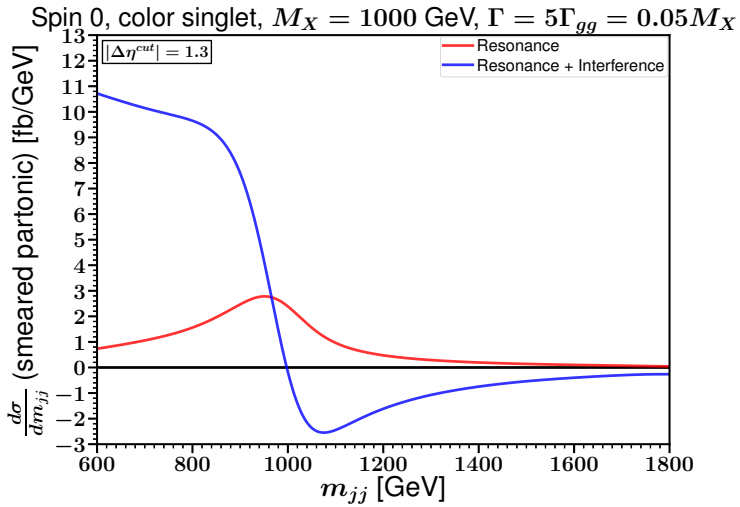

$M_X = 3000$ GeV:

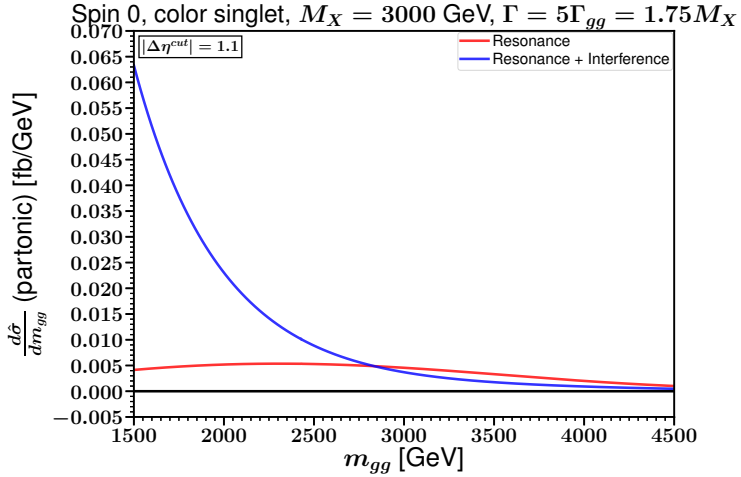

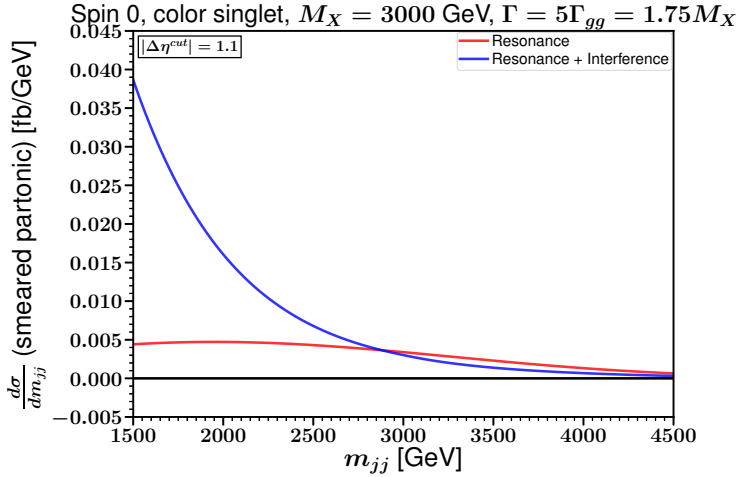

Results for $\Gamma = 5\Gamma_{gg}$: Spin 0, color octet (parton-level approximation)

$M_X = 1000$ GeV:

Partonic

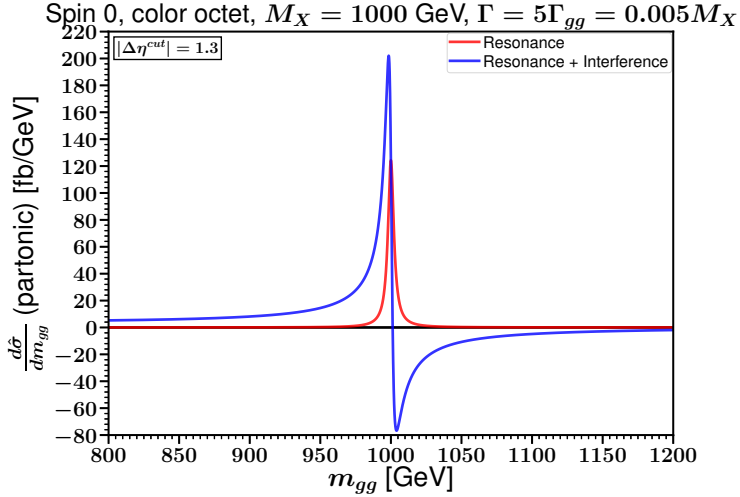

Smeared partonic

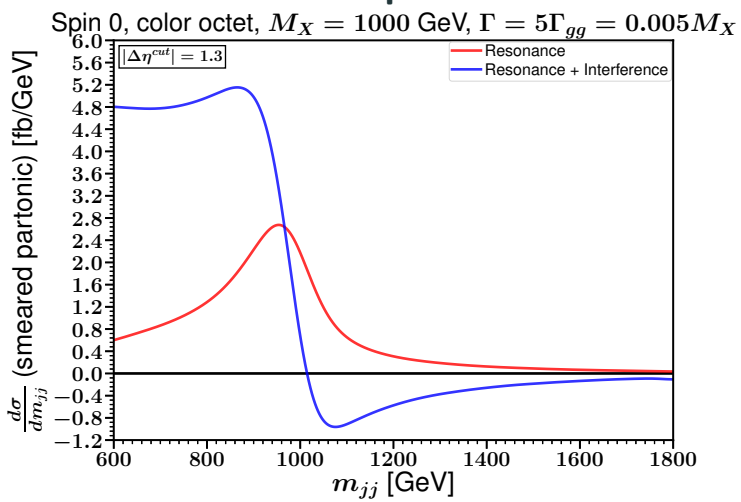

$M_X = 3000$ GeV:

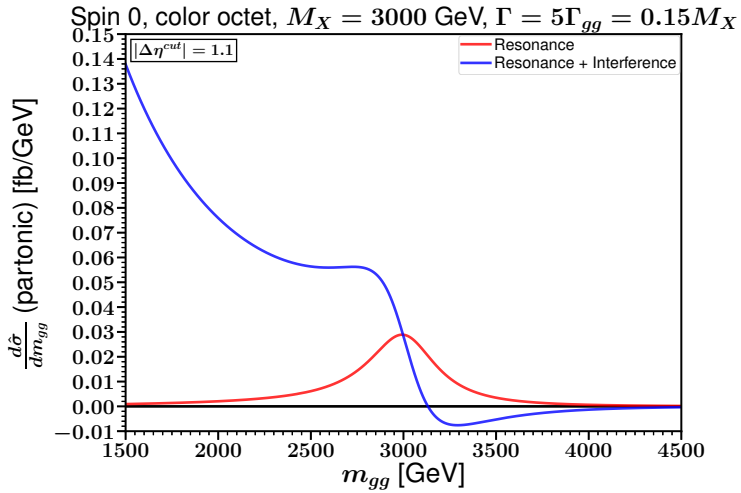

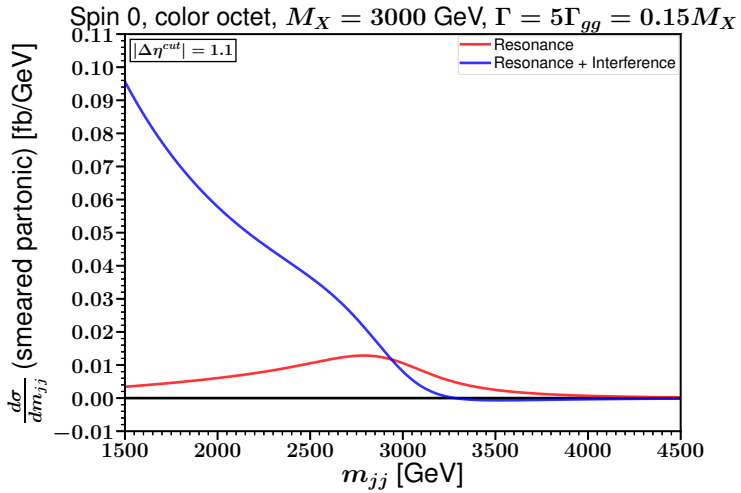

Results for $\Gamma = 5\Gamma_{gg}$: Spin 1, color octet (parton-level approximation)

$M_X = 1000$ GeV:

Partonic

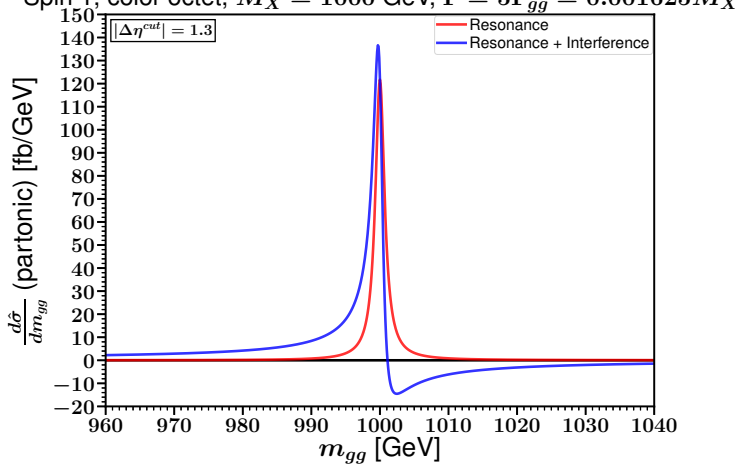

Smeared partonic

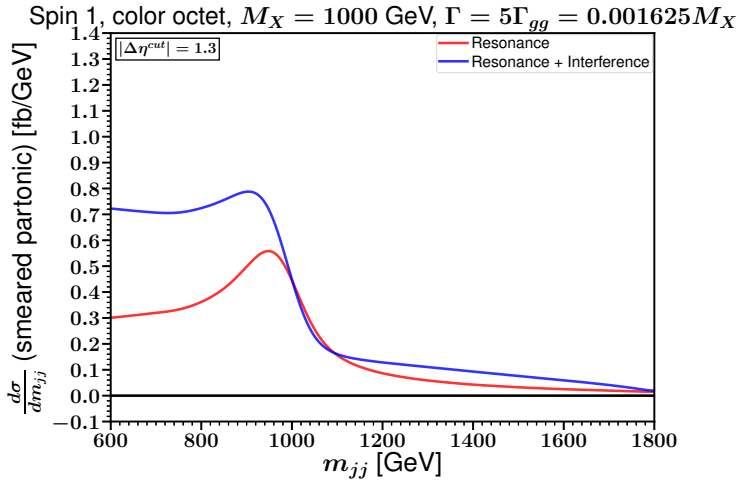

$M_X = 3000$ GeV:

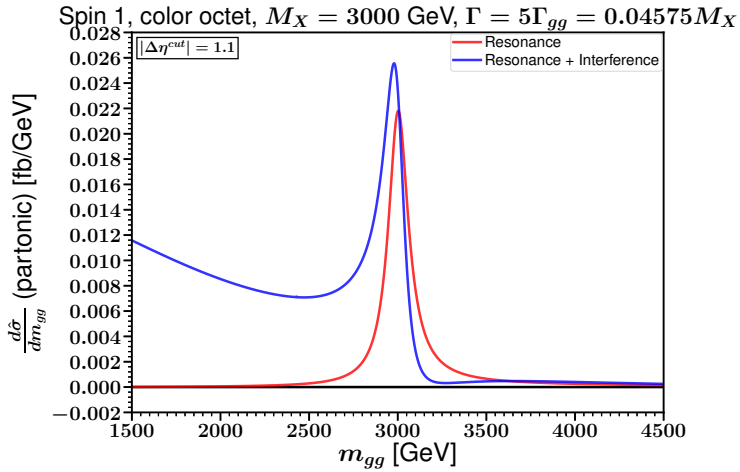

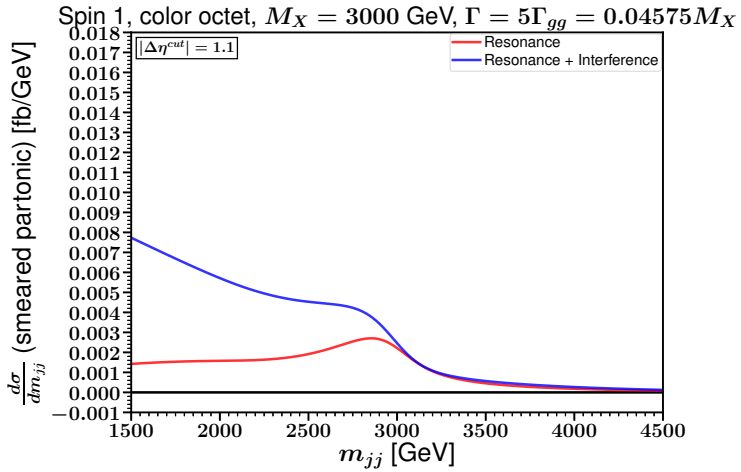

Results for $\Gamma = 5\Gamma_{gg}$: Spin 2, color singlet (parton-level approximation)

$M_X = 1000$ GeV:

Partonic

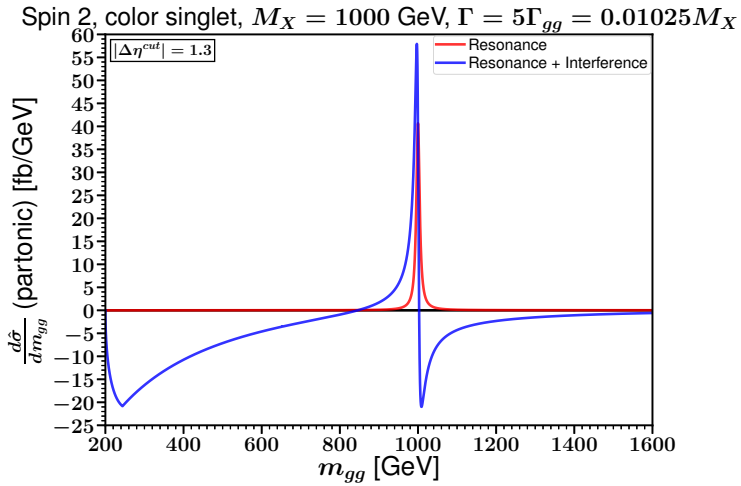

Smeared partonic

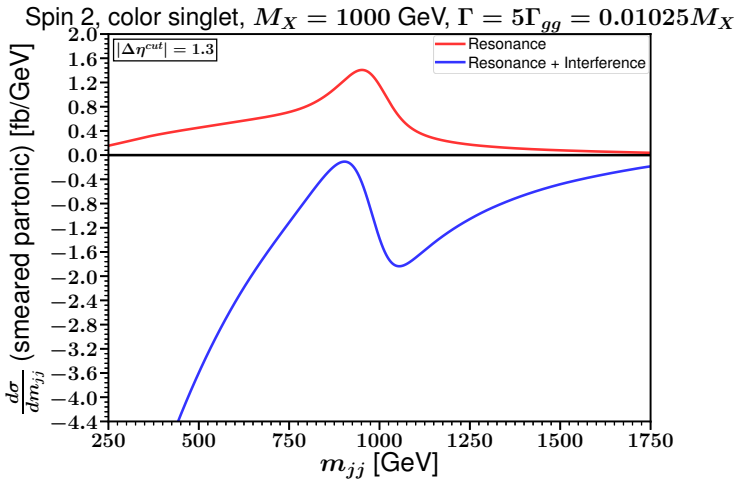

$M_X = 3000$ GeV:

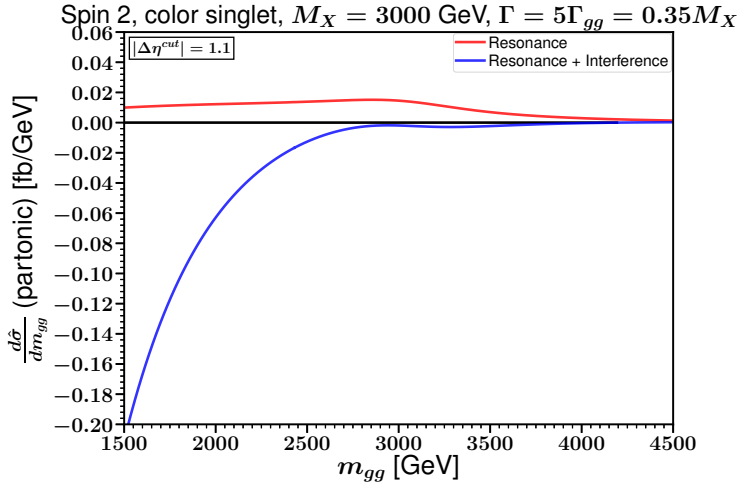

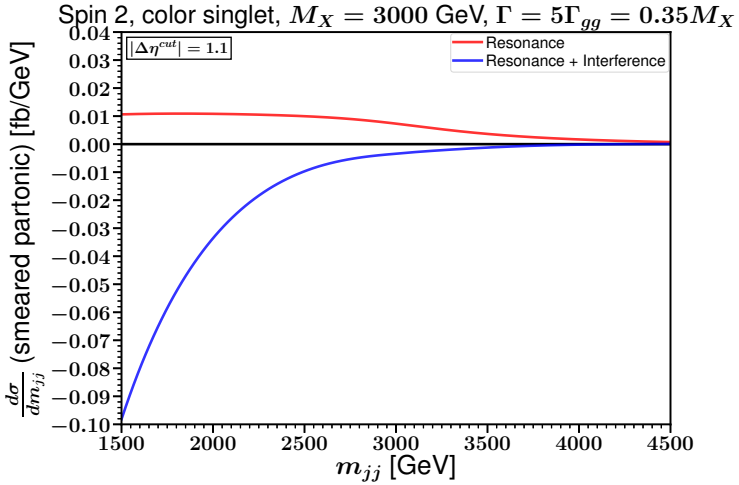

Discussions for $\Gamma = 5\Gamma_{gg}$

- The interference effects are relatively enhanced compared to the case with $\Gamma = \Gamma_{gg}$. The distributions including interference can bear little resemblance to the naive resonance-only results.
- In each of the spin-0 and spin-1 cases, there is a very large low-mass tail from the interference. For lower M_X and spin-0, we find a pronounced dip for m_{jj} above M_X, but this tends to be washed out for larger M_X and higher spin.
- The falling distributions well below M_X, if present, could result in a peak/dip or dip shape after fitting to the QCD background. The magnitude of the effective dip could be as large or larger than the naive resonance peak.
- In the spin-2 color-singlet case, the distribution shape tends to feature a large deficit at low masses, a peak just below M_X, and then another deficit above M_X. After fitting the QCD background, this should lead to an enhancement of the peak compared to the naive resonance-only distribution.